IMA Journal of Numerical Analysis (2022) **42**, 2505–2544
https://doi.org/10.1093/imanum/drab044
Advance Access publication on 5 July 2021

An unfitted Eulerian finite element method for the time-dependent Stokes problem on moving domains

Henry von Wahl* and Thomas Richter
Institut für Analysis und Numerik, Otto-von-Guericke-Universität, Universitätsplatz 2, D-39106 Magdeburg, Germany
*Corresponding author: henry.vonwahl@ovgu.de

and

Christoph Lehrenfeld
Institut für Numerische und Angewandte Mathematik, Georg-August-Universität Göttingen, Lotzestraße 16-18, D-37083 Göttingen, Germany

[Received on 11 February 2020; revised on 5 November 2020]

We analyse a Eulerian finite element method, combining a Eulerian time-stepping scheme applied to the time-dependent Stokes equations with the CutFEM approach using inf-sup stable Taylor–Hood elements for the spatial discretization. This is based on the method introduced by Lehrenfeld & Olshanskii (2019, A Eulerian finite element method for PDEs in time-dependent domains. *ESAIM: M2AN*, **53**, 585–614) in the context of a scalar convection–diffusion problems on moving domains, and extended to the nonstationary Stokes problem on moving domains by Burman *et al.* (2019, arXiv:1910.03054 [math.NA]) using stabilized equal-order elements. The analysis includes the geometrical error made by integrating over approximated level set domains in the discrete CutFEM setting. The method is implemented and the theoretical results are illustrated using numerical examples.

1. Introduction

Flow problems on time-dependent domains are important in many different applications in biology, physics and engineering, such as blood flows (Ambrosi *et al.*, 2012) or fluid–structure interaction problems (Richter, 2017), e.g., freely moving solids submersed in a fluid or generally in multi-phase flow applications, e.g., coupling a liquid and gas.

The most well-established methods for these kind of problems studied in the literature are either based at least partially on a Lagrangian or a purely Eulerian description of the domain boundary and its motion. Famous are arbitrary Lagrangian–Eulerian (ALE) methods (Donea *et al.*, 1982, 2004), which can be combined with standard time-stepping schemes or space–time Galerkin formulations (Behr, 2001, 2008; Klaij *et al.*, 2006; Neumüller, 2013). ALE methods rely on geometry-fitted moving meshes or space–time meshes. The motion of corresponding meshes and their necessary adaptations after significant geometry deformations can be a severe burden for those methods, depending on the amount of geometrical change. To circumvent the problem of regular mesh updates or space–time meshing Eulerian methods can be considered. This is also the approach taken in this paper. Here, a static computational background mesh is used to define potential unknowns and the geometry is incorporated separately. In the context of finite element methods (FEM) these *unfitted* FEMs have become popular within the past decade and are known under different names, e.g., XFEM (Fries & Belytschko, 2010), CutFEM (Burman *et al.*, 2014), finite cell method (Parvizian *et al.*, 2007) and TraceFEM (Olshanskii *et al.*, 2009). Similar concepts have also been used before, e.g., in penalty methods (Babuska, 1973; Barrett & Elliott, 1986), the fictitious domain method (Glowinski *et al.*, 1994a,b) and the immersed boundary method (Peskin & McQueen, 1989). While these methods reached a considerable level of maturity for stationary problems, problems with moving geometries—one of the main targets for unfitted FEMs—are not well established. This is due to the fact that standard time-stepping approaches are not straight-forwardly applicable in a Eulerian framework, where the expression $\partial_t \boldsymbol{u} \approx \Delta t^{-1}(\boldsymbol{u}^n - \boldsymbol{u}^{n-1})$ is not well defined if $\boldsymbol{u}^n$ and $\boldsymbol{u}^{n-1}$ live on different domains.

One approach that has been proven to work despite this inconvenient setting is the class of space–time Galerkin formulations in a Eulerian setting, as they have been considered in Lehrenfeld & Reusken (2013), Lehrenfeld (2015), Preuß (2018), Zahedi (2018) for scalar bulk problems, on moving surfaces in Grande *et al.* (2014), Olshanskii & Reusken (2014), Olshanskii *et al.* (2014) or for surface-bulk coupled problems in Hansbo *et al.* (2016). Recently, also preliminary steps towards unfitted space–time finite elements for two-phase flows have been addressed in Voulis & Reusken (2018), Anselmann & Bause (2020). These methods however have the disadvantage that one has to deal with—in one way or another—a higher dimensional problem. Using an adjusted quadrature rule to reduce the space–time formulation to a classical time stepping scheme as in Frei & Richter (2017) requires costly computations of projections between discrete function spaces at times t_{n-1} and t_n.

In the following we consider an alternative to space–time methods, which allows for a more standard time-stepping structure. This has been introduced in Lehrenfeld *et al.* (2018), Lehrenfeld & Olshanskii (2019) and considered for flow problems in Burman *et al.* (2019). To discretize the time derivative in the spatially smooth setting, the method applies a standard method-of-lines approach using a backward-differentiation formula in combination with a continuous extension operator in Sobolev spaces. This extension ensures that the previous solution defined on the domain $\Omega(t_{n-1})$ has meaning on the domain $\Omega(t_n)$. In the fully discrete setting, the approach uses an unfitted FEM on a fixed background mesh to discretize the domain, and applies additional stabilization outside the physical domain, such that the discrete solution has meaning on a larger domain $\mathcal{O}(\Omega_h(t_{n-1})) \supset \Omega_h(t_n)$. The major challenge with this approach, in the context of fluid problems, is that the velocities at different time points, are weakly divergence free with respect to different pressure spaces. This means that the approximated time-derivative $\Delta t^{-1}(\boldsymbol{u}_h^n - \boldsymbol{u}_h^{n-1})$ is not weakly divergence free, which causes stability problems for the pressure, as is known from the case of fitted methods and stationary domains (Besier & Wollner, 2011; Brenner *et al.*, 2013).

The essential idea, to extend the discrete fluid velocity solution onto the active mesh at the next time step using ghost penalties, in order to use a method-of-lines approach for the discretization of the time derivative, has also been considered in Schott (2017, Section 3.6.3). However, there the extension of the velocity solution has been split into a separate substep, and has been limited to the extension to a vertex patch of previously active elements, such that the time step must obey a Courant-Friedrichs-Lewy (CFL) condition $\Delta t \leq ch$. Furthermore, the analysis of this split approach currently remains open.

In the recent work by Burman *et al.* (2019), the implicit extension technique introduced in Lehrenfeld & Olshanskii (2019) was also considered for the time-dependent Stokes problem on moving domains. Here, the spatial discretization consists of equal-order pressure stabilized unfitted finite elements. The present paper differs from Burman *et al.* (2019) in the following aspects. As an underlying Stokes discretization we consider the inf-sup stable Taylor-Hood velocity-pressure pairing, pressure stabilization is therefore only applied in the vicinity of the domain boundary. In contrast to Burman *et al.* (2019), we consider the general case where geometrical approximation errors are considered and included in the error analysis. Furthermore, we allow the geometry to surpass several element layers within one time step without introducing a CFL-like condition, and consider not only the case of viscosities that are of order 1.

The remainder of this paper is structured as follows. In Section 2 we formally describe the smooth problem we aim to solve numerically. We then begin with the temporal semidiscretization of the smooth problem in Section 3, where we also show the stability of the approach in the spatially smooth setting. Section 4 then covers the description of the fully discrete problem, including the stabilization operator that realizes the discrete extension in the method. The main part of this paper is then the fully discrete analysis of the method in Section 5. Here wo go into the details of how the geometrical consistency error, inherent in unfitted FEMs using level sets, affects the coupling of the velocity and pressure errors. We then present numerical examples for the method in Section 6. Here we show the dominance of the geometrical error in practice, as well as discussing approaches to avoid this issue. Furthermore, we show the robustness of our method over a wide range of viscosities. Finally, in Section 7, we then discuss the conclusions from this work and discuss remaining open problems connected to this method.

2. Problem description

Let us consider a time-dependent domain $\Omega(t) \subset \mathbb{R}^d$ with $d \in \{2, 3\}$ and Lipschitz continuous boundary $\Gamma(t) = \partial\Omega(t)$ over a fixed and bounded time-interval $[0, T]$, and assume that this domain evolves smoothly in time. We then define the space–time domain as $\mathcal{Q} := \bigcup_{t\in(0,T)} \Omega(t) \times \{t\}$. In $\mathcal{Q}$ we then consider the time-dependent Stokes problem: find the velocity $\boldsymbol{u}$ and pressure p, such that

$$\partial_t \boldsymbol{u} - \nu\Delta\boldsymbol{u} + \nabla p = \boldsymbol{f} \tag{2.1a}$$
$$\nabla \cdot \boldsymbol{u} = 0 \tag{2.1b}$$

together with homogeneous Dirichlet boundary conditions on the space boundary, initial condition $\boldsymbol{u}(0) = \boldsymbol{u}_0$ and a forcing term $\boldsymbol{f}(t)$ with the viscosity $\nu > 0$. For the well posedness of this problem we refer to (Burman *et al.*, 2019, Section 2.1).

The following analysis calls for substantial assumptions on the solution's regularity, namely

$$\boldsymbol{u} \in \boldsymbol{\mathcal{L}}^\infty(0, T; \boldsymbol{\mathcal{H}}^{m+1}(\Omega(t))) \cap \boldsymbol{\mathcal{W}}^{2,\infty}(\mathcal{Q}), \quad \boldsymbol{u}_t \in \boldsymbol{\mathcal{L}}^\infty(0, T; \boldsymbol{\mathcal{H}}^m(\Omega(t))), \quad p \in \mathcal{L}^\infty(0, T; \mathcal{H}^m(\Omega(t))),$$

where m is the polynomial degree of the finite element space. For $1 \le m \le 8$ this requirement is dominated by $\boldsymbol{u} \in \boldsymbol{\mathcal{W}}^{2,\infty}(\mathcal{Q})$. To reach this high regularity Temem (1982, Theorem 2.1 and Theorem 2.2), who covers the case of fixed domains, states the exact conditions for initial data and right-hand side as

$$\boldsymbol{u}_0 \in \boldsymbol{\mathcal{H}}^{10}(\Omega), \quad \frac{d^l\boldsymbol{f}}{dt^l} \in \boldsymbol{\mathcal{L}}^\infty(0, T; \boldsymbol{\mathcal{H}}^{8-2l}(\Omega)),\ l = 0, \dots, 4,$$

a domain with C^{10}-boundary and, in addition, nonlocal compatibility conditions for the pressure at time $t \to 0$. To overcome these compatibility conditions, which are usually impossible to validate, one would have to exploit smoothing estimates by considering weighted norms, see Heywood & Rannacher (1990) or Sonner & Richter (2020) with a focus on the pressure regularity.

3. Time discretization

For simplicity let us consider a uniform time-step $\Delta t = T/N$ for some fixed $N \in \mathbb{N}$. We then denote $t_n = n\Delta t$, $I_n = [t_{n-1}, t_n)$, $\Omega^n = \Omega(t_n)$ and $\Gamma^n = \Gamma(t_n)$. We define the δ-neighbourhood of $\Omega(t)$ as

$$\mathcal{O}_\delta(\Omega(t)) := \{\boldsymbol{x} \in \mathbb{R}^d \mid \operatorname{dist}(\boldsymbol{x}, \Omega(t)) \leq \delta\}.$$

For our method we require that the domain Ω^n lies within the δ-neighbourhood of the previous domain, i.e.,

$$\Omega^n \subset \mathcal{O}_\delta(\Omega^{n-1}), \quad \text{for } n = 1, \ldots, N.$$

We ensure that this requirement is fulfilled by the choice

$$\delta = c_\delta w_\infty^n \Delta t,$$

where w_∞^n is the maximal normal speed of the domain interface and $c_\delta > 1$.

The time discretization is then based on a *method of lines* approach, in combination with an extension operator for Sobolev functions to a δ-neighbourhood, which ensures that solutions defined on domains at previous time steps are well defined on Ω^n. See Section 3.1.3 for details of this extension operator.

3.1 *Variational formulation*

3.1.1 *Notation.* We introduce some notation. By $\mathcal{L}^2(S)$ we denote the function space of square integrable functions on a domain S while $\mathcal{H}^1(S)$ is the usual Sobolev space of functions in $\mathcal{L}^2(S)$, which have first-order weak derivatives in $\mathcal{L}^2(S)$. We define the subspace of $\mathcal{L}^2(S)$ of functions with mean value zero $\mathcal{L}^2_0(S) := \{v \in \mathcal{L}^2(S) \mid \int_S v \,\mathrm{d}\boldsymbol{x} = 0\}$ and the subspace of $\mathcal{H}^1(S)$ of functions with zero boundary values (in the trace sense) as $\mathcal{H}^1_0(S)$. The dual space to $(\mathcal{H}^1_0(S), \|\nabla \cdot\|_S)$ is denoted by $\mathcal{H}^{-1}(S)$. For vector-valued functions we write these spaces bold. Further, we introduce the Poincaré constant $c_P > 0$, which ensures that for all $v \in \mathcal{H}^1_0(\Omega(t))$ and all $t \in (0, T)$ there holds $\|v\|_{\Omega(t)} \leq c_P \|\nabla v\|_{\Omega(t)}$.

3.1.2 *Semidiscretization.* We discretize the time derivative with the implicit Euler (or BDF1) method in combination with the extension operator. Multiplying (2.1) with a test function, integrating over Ω^n and using integration by parts to obtain the weak formulations for the diffusion and velocity-pressure coupling terms the variational formulation of the temporally semidiscrete problem then reads: for $n = 1, \ldots, N$, given $\boldsymbol{u}^{n-1} \in \boldsymbol{\mathcal{H}}^1_0(\Omega^{n-1})$ and $\boldsymbol{f}^n \in \boldsymbol{\mathcal{H}}^{-1}(\Omega^n)$, find $(\boldsymbol{u}^n, p^n) \in \boldsymbol{V}^n \times Q^n := \boldsymbol{\mathcal{H}}^1(\Omega^n) \times \mathcal{L}^2_0(\Omega^n)$ such that for all $(\boldsymbol{v}, q) \in \boldsymbol{V}^n \times Q^n$ it holds

$$\frac{1}{\Delta t}(\boldsymbol{u}^n, \boldsymbol{v})_{\Omega^n} + a^n(\boldsymbol{u}^n, \boldsymbol{v}) + b^n(p^n, \boldsymbol{v}) + b^n(q, \boldsymbol{u}^n) = \langle \boldsymbol{f}^n, \boldsymbol{v}\rangle_{(\boldsymbol{V}^n)', \boldsymbol{V}^n} + \frac{1}{\Delta t}(\mathcal{E}\boldsymbol{u}^{n-1}, \boldsymbol{v})_{\Omega^n}. \tag{3.1}$$

Here, $(\cdot,\cdot)_{\Omega^n}$ denotes the $\boldsymbol{\mathcal{L}}^2$-inner product and the bilinear forms are

$$a^n(\boldsymbol{u}, \boldsymbol{v}) = \nu \int_{\Omega^n} \nabla \boldsymbol{u} : \nabla \boldsymbol{v} \,\mathrm{d}\boldsymbol{x} \quad \text{and} \quad b^n(q, \boldsymbol{v}) = -\int_{\Omega^n} q \nabla \cdot \boldsymbol{v} \,\mathrm{d}\boldsymbol{x} \tag{3.2}$$

for the diffusion term and the velocity–pressure coupling, respectively. $\mathcal{E} : \boldsymbol{\mathcal{H}}^1(\Omega^{n-1}) \to \boldsymbol{\mathcal{H}}^1(\mathcal{O}_\delta(\Omega^{n-1}))$ is the extension operator—discussed in the next section—that allows us to make sense of the 'initial value' $\boldsymbol{u}^{n-1} \in \boldsymbol{\mathcal{H}}^1_0(\Omega^{n-1})$ in $\Omega^n \subset \mathcal{O}_\delta(\Omega^{n-1})$.

3.1.3 *Extension operator.* For the extension operator we require the following family of space–time anisotropic spaces

$$\boldsymbol{\mathcal{L}}^\infty(0,T;\boldsymbol{\mathcal{H}}^k(\Omega(t))) := \left\{ \boldsymbol{v} \in \boldsymbol{\mathcal{L}}^2(\mathcal{Q}) \,\middle|\, \begin{array}{r} \boldsymbol{v}(\cdot,t) \in \boldsymbol{\mathcal{H}}^k(\Omega(t)) \text{ for a.e. } t \in (0,T) \\ \text{and } \operatorname{ess\,sup}_{t\in(0,T)} \|\boldsymbol{v}(\cdot,t)\|_{\boldsymbol{\mathcal{H}}^k(\Omega(t))} < \infty \end{array} \right\}$$

for $k = 0,\dots,m+1$. We then denote $\partial_t \boldsymbol{v} = \boldsymbol{v}_t$ as the weak partial derivative with respect to the time variable, if this exists as an element in the space–time space $\boldsymbol{\mathcal{L}}^2(\mathcal{Q})$. We also use the standard notation for $\mathcal{L}^2$-norms of $\|\cdot\|_S = \|\cdot\|_{\mathcal{L}^2(S)}$ for some domain S.

We now assume the existence of a spatial extension operator

$$\mathcal{E} : \boldsymbol{\mathcal{L}}^2(\Omega(t)) \to \boldsymbol{\mathcal{L}}^2(\mathcal{O}_\delta(\Omega(t))),$$

which fulfils the following properties:

Assumption A1 Let $\boldsymbol{v} \in \boldsymbol{\mathcal{L}}^\infty(0,T;\boldsymbol{\mathcal{H}}^{m+1}(\Omega(t))) \cap \boldsymbol{\mathcal{W}}^{2,\infty}(\mathcal{Q})$. There exist positive constants $c_{A1\mathrm{a}}$, $c_{A1\mathrm{b}}$ and $c_{A1\mathrm{c}}$ that are uniform in t, such that

$$\|\mathcal{E}\boldsymbol{v}\|_{\boldsymbol{\mathcal{H}}^k(\mathcal{O}_\delta(\Omega(t)))} \le c_{A1\mathrm{a}} \|\boldsymbol{v}\|_{\boldsymbol{\mathcal{H}}^k(\Omega(t))} \tag{3.3a}$$

$$\|\nabla(\mathcal{E}\boldsymbol{v})\|_{\mathcal{O}_\delta(\Omega(t))} \le c_{A1\mathrm{b}} \|\nabla \boldsymbol{v}\|_{\Omega(t)} \tag{3.3b}$$

$$\|\mathcal{E}\boldsymbol{v}\|_{\boldsymbol{\mathcal{W}}^{2,\infty}(\mathcal{O}_\delta(\mathcal{Q}))} \le c_{A1\mathrm{c}} \|\boldsymbol{v}\|_{\boldsymbol{\mathcal{W}}^{2,\infty}(\mathcal{Q})} \tag{3.3c}$$

holds. Furthermore, if for $\boldsymbol{v} \in \boldsymbol{\mathcal{L}}^\infty(0,T;\boldsymbol{\mathcal{H}}^{m+1}(\Omega(t)))$ it holds for the weak partial time derivative that $\boldsymbol{v}_t \in \boldsymbol{\mathcal{L}}^\infty(0,T;\boldsymbol{\mathcal{H}}^m(\Omega(t)))$, then

$$\|(\mathcal{E}\boldsymbol{v})_t\|_{\boldsymbol{\mathcal{H}}^m(\mathcal{O}_\delta(\Omega(t)))} \le c_{A1\mathrm{d}} \left[\|\boldsymbol{v}\|_{\boldsymbol{\mathcal{H}}^{m+1}(\Omega(t))} + \|\boldsymbol{v}_t\|_{\boldsymbol{\mathcal{H}}^m(\Omega(t))} \right], \tag{3.4}$$

where the constant $c_{A1\mathrm{d}} > 0$ again only depends on the motion of the spatial domain.

Remark 3.1 Such an extension operator can be constructed explicitly from the classical linear and continuous *universal* extension operator for Sobolev spaces (see e.g., Stein, 1970, Section VI.3), when the motion of the domain can be described by a diffeomorphism $\Psi(t) : \Omega_0 \to \Omega(t)$ for each $t \in [0,T]$ from the reference domain Ω_0 that is smooth in time. See Lehrenfeld & Olshanskii (2019) for details thereof.

Assuming sufficient regularity of the domain Ω^n, e.g., connected with Lipschitz boundary, well posedness of (3.1) is given for every time step by the standard theory of the Stokes–Brinkman problem, or equivalently the Oseen problem with vanishing convective velocity, see for example John (2016, Theorem 5.7).

3.2 *Stability*

We now show that the semidiscrete scheme (3.1) gives a stable solution for both the velocity and pressure.

LEMMA 3.2 Let $\{\boldsymbol{u}^n\}_{n=1}^N$ be the velocity solution of (3.1) with initial data $\boldsymbol{u}^0 \in \boldsymbol{\mathcal{H}}^1(\Omega^0)$. Then it holds that

$$\|\boldsymbol{u}^k\|_{\Omega^k}^2 + \Delta t \sum_{n=1}^{k} \frac{\nu}{2} \|\nabla \boldsymbol{u}^n\|_{\Omega^n}^2 \leq \exp(c_{L3.2} t_k) \left[\|\boldsymbol{u}^0\|_{\Omega^0}^2 + \frac{\nu \Delta t}{2} \|\nabla \boldsymbol{u}^0\|_{\Omega^0}^2 + \frac{c_P^2 \Delta t}{\nu} \sum_{n=1}^{k} \|\boldsymbol{f}^n\|_{\Omega^n}^2 \right]$$

with a constant $c_{L3.2}$ independent of the time step Δt and the number of steps k.

Proof. The proof is analog to that of Lehrenfeld & Olshanskii (2019, Lemma 3.6) with the different choice of test-function $2\Delta t(\boldsymbol{u}^n, -p^n) \in \boldsymbol{V}^n \times Q^n$ to remove the pressure from the equation. □

LEMMA 3.3 Let $\{p^n\}_{n=1}^N$ be the pressure solution of (3.1). Then it holds that

$$\|p^n\|_{\Omega^n} \leq \frac{1}{\beta} \left(c_P \|\boldsymbol{f}^n\|_{\Omega^n} + \frac{1}{\Delta t} \|\boldsymbol{u}^n - \mathcal{E}\boldsymbol{u}^{n-1}\|_{\boldsymbol{\mathcal{H}}^{-1}(\Omega^n)} + \nu \|\nabla \boldsymbol{u}^n\|_{\Omega^n} \right) \tag{3.5}$$

with a constant $\beta > 0$ bounded independent of Δt.

Proof. Let β^n be the inf-sup constant of the space pair $\boldsymbol{V}^n \times Q^n = \boldsymbol{\mathcal{H}}_0^1(\Omega^n) \times \mathcal{L}_0^2(\Omega^n)$ and denote $\beta = \min_{n=0,\ldots,N} \beta^n$. From the inf-sup stability of the velocity and pressure spaces and, by rewriting the momentum balance equation, it follows that

$$\beta \|p^n\|_{\Omega^n} \leq \beta^n \|p^n\|_{\Omega^n} \leq \sup_{\boldsymbol{v} \in \boldsymbol{V}^n} \frac{b^n(p^n, \boldsymbol{v})}{\|\nabla \boldsymbol{v}\|_{\Omega^n}} = \sup_{\boldsymbol{v} \in \boldsymbol{V}^n} \frac{(\boldsymbol{f}^n, \boldsymbol{v})_{\Omega^n} - \frac{1}{\Delta t}(\boldsymbol{u}^n - \mathcal{E}\boldsymbol{u}^{n-1}, \boldsymbol{v})_{\Omega^n} - a^n(\boldsymbol{u}^n, \boldsymbol{v})}{\|\nabla \boldsymbol{v}\|_{\Omega^n}}.$$

Taking absolute values, applying Cauchy–Schwarz and using the Poincaré inequality and the continuity of the diffusion bilinear form we get the claim. □

REMARK 3.4 At first glance it seems unclear if the estimate in (3.5) yields a pressure bound that is independent of Δt. Let us explain why a scaling of $\|p^n\|_{\Omega^n}$ with Δt^{-1} is not to be expected. The argument is based on an a relation for the discretization error. The exact solution $(\boldsymbol{u}(t_n), p(t_n))$ fulfils for all $\boldsymbol{v} \in \boldsymbol{V}^n$ and all $q \in Q^n$ an equation similar to (3.1):

$$\left(\partial_t \boldsymbol{u}(t_n), \boldsymbol{v}\right)_{\Omega^n} + a^n(\boldsymbol{u}(t_n), \boldsymbol{v}) + b^n(p(t_n), \boldsymbol{v}) + b^n(q, \boldsymbol{u}(t_n)) = \langle \boldsymbol{f}^n, \boldsymbol{v} \rangle_{(\boldsymbol{V}^n)', \boldsymbol{V}^n}.$$

We find for $\mathbb{E}^k := \boldsymbol{u}(t_k) - \boldsymbol{u}^k$, and $\mathbb{D}^k := p(t_k) - p^k$, $k = 1, .., N$ that there holds

$$\left(\frac{\mathbb{E}^n - \mathcal{E}\mathbb{E}^{n-1}}{\Delta t}, \boldsymbol{v} \right)_{\Omega^n} + a^n(\mathbb{E}^n, \boldsymbol{v}) + b^n(\mathbb{D}^n, \boldsymbol{v}) + b^n(q, \mathbb{E}^n) = \left(\frac{\boldsymbol{u}(t_n) - \mathcal{E}\boldsymbol{u}(t_{n-1})}{\Delta t} - \partial_t \boldsymbol{u}(t_n), \boldsymbol{v} \right)_{\Omega^n}$$

for all $\boldsymbol{v} \in \boldsymbol{V}^n$ and $q \in Q^n$. Now, assuming sufficient regularity, i.e., $u \in \boldsymbol{\mathcal{W}}^{2,\infty}(\mathcal{Q})$, we easily obtain the bound $c_{R3.4\mathrm{a}} \Delta t \|\boldsymbol{u}\|_{\boldsymbol{\mathcal{W}}^{2,\infty}(\mathcal{Q})} \|\boldsymbol{v}\|_{\Omega^n}$ for the r.h.s. with a constant $c_{R3.4\mathrm{a}}$ independent of n, $\boldsymbol{u}$ and Δt. Here, we also made use of (3.3c). As the l.h.s. is the same as in (3.1) we can apply Lemma 3.3 (using $\mathbb{E}^0 = 0$) to obtain the bound

$$\|\mathbb{E}^n\|_{\Omega^n} \leq c_{R3.4\mathrm{b}} \exp(c_{R3.4\mathrm{c}} t_n) \Delta t \|\boldsymbol{u}\|_{\boldsymbol{\mathcal{W}}^{2,\infty}(Q)}.$$

Hence, a simple triangle inequality yields

$$\begin{aligned}\frac{1}{\Delta t}\|\boldsymbol{u}^n - \mathcal{E}\boldsymbol{u}^{n-1}\|_{\boldsymbol{\mathcal{H}}^{-1}(\Omega^n)} &\leq \frac{1}{\Delta t}\|\boldsymbol{u}(t_n) - \mathcal{E}\boldsymbol{u}(t_{n-1})\|_{\boldsymbol{\mathcal{H}}^{-1}(\Omega^n)} + \frac{1}{\Delta t}\|\mathbb{E}^n\|_{\boldsymbol{\mathcal{H}}^{-1}(\Omega^n)} + \frac{1}{\Delta t}\|\mathcal{E}\mathbb{E}^{n-1}\|_{\boldsymbol{\mathcal{H}}^{-1}(\Omega^n)}\\ &\leq \|\partial_t \boldsymbol{u}(t_n)\|_{\boldsymbol{\mathcal{H}}^{-1}(\Omega^n)} + c_{R3.4\mathrm{d}} \Delta t \|\boldsymbol{u}\|_{\boldsymbol{\mathcal{W}}^{2,\infty}(Q)},\end{aligned}$$

and hence a bound on the norm of p^n that is independent on Δt^{-1}.

4. The fully discrete method

For the spatial discretization of the method we use the CutFEM approach (Burman *et al.*, 2014). Within the CutFEM framework we consider a background domain $\widetilde{\Omega} \subset \mathbb{R}^d$ and assume that $\Omega(t) \subset \widetilde{\Omega}$ for all $t \in [0, T]$. We then take a simplicial, shape-regular and quasi-uniform mesh $\widetilde{\mathcal{T}_h}$ of $\widetilde{\Omega}$, where $h > 0$ is the characteristic size of the simplices. Bad cuts of the mesh with the domain boundary $\Gamma(t)$ are stabilized using ghost-penalty stabilization (Burman, 2010). We will discuss the details of this in Section 4.1.1. The fully discrete method realizes the necessary extension implicitly, by applying the ghost-penalty stabilization operation on a larger extension region when solving for the solution in each time step. At each time step we therefore extend the (discrete) physical domain Ω_h^n by a strip of width

$$\delta_h = c_{\delta_h} w_\infty^n \Delta t$$

such that Ω_h^{n+1} is a subset of this extended domain with $c_{\delta_h} > 1$, but sufficiently small so that $\mathcal{O}_{\delta_h}(\Omega_h^n) \subset \mathcal{O}_\delta(\Omega^n)$. We collect all elements that have some part in this extended domain at time $t = t_n$ in the *active velocity mesh*, denoted as

$$\mathcal{T}_{h,\delta_h}^n := \{K \in \widetilde{\mathcal{T}_h} \mid \exists \boldsymbol{x} \in K \text{ such that } \mathrm{dist}(\boldsymbol{x}, \Omega_h^n) \leq \delta_h\} \subset \widetilde{\mathcal{T}_h}$$

and denote the *active domain* as

$$\mathcal{O}_{\delta_h,\mathcal{T}}^n := \{\boldsymbol{x} \in K \mid K \in \mathcal{T}_{h,\delta_h}\} \subset \mathbb{R}^d.$$

We further define the *cut mesh* as $\mathcal{T}_h^n = \mathcal{T}_{h,0}^n$ of all elements that contain some part of the physical domain and the *cut domain* as $\mathcal{O}_{\mathcal{T}}^n = \mathcal{O}_{0,\mathcal{T}}^n$.

On the active mesh we consider an inf-sup stable finite element pair $\boldsymbol{V}_h \times Q_h$ for the Nitsche–CutFEM discretization of the Stokes problem (Burman & Hansbo, 2014; Massing *et al.*, 2014). For an overview of such elements see Guzmán & Olshanskii (2017). We shall use the family of Taylor–Hood finite elements for $k \geq 2$

$$\boldsymbol{V}_h^n := \{\boldsymbol{v}_h \in \boldsymbol{C}(\mathcal{O}_{\delta_h,\mathcal{T}}^n) \mid \boldsymbol{v}_h\big|_K \in [\mathbb{P}^k(K)]^d \text{ for all } K \in \mathcal{T}_{h,\delta_h}^n\}$$

and

$$Q_h^n := \left\{ q_h \in C(\mathcal{O}_{\mathcal{T}}^n) \mid \boldsymbol{v}_h\big|_K \in \mathbb{P}^{k-1}(K) \text{ for all } K \in \mathcal{T}_h^n \right\}.$$

4.1 *The variational formulation*

The fully discrete variational formulation of the method reads as follows: given an appropriate initial condition $\boldsymbol{u}_h^0 \in \boldsymbol{V}_h^0$, for $n = 1, \dots, N$ find $(\boldsymbol{u}_h^n, p_h^n) \in \boldsymbol{V}_h^n \times Q_h^n$, such that

$$\int_{\Omega_h^n} \frac{\boldsymbol{u}_h^n - \boldsymbol{u}_h^{n-1}}{\Delta t} \cdot \boldsymbol{v}_h \, \mathrm{d}\boldsymbol{x} + a_h^n(\boldsymbol{u}_h^n, \boldsymbol{v}_h) + b_h^n(p_h^n, \boldsymbol{v}_h) + b_h^n(q_h, \boldsymbol{u}_h^n) + s_h^n((\boldsymbol{u}_h^n, p_h^n), (\boldsymbol{v}_h, q_h)) = \boldsymbol{f}_h^n(\boldsymbol{v}_h) \quad (4.1)$$

for all $(\boldsymbol{v}_h, q_h) \in \boldsymbol{V}_h^n \times Q_h^n$. We impose the homogeneous Dirichlet boundary conditions in a weak sense using the symmetric Nitsches method (Nitsche, 1971). For the diffusion term the bilinear form is then

$$a_h^n(\boldsymbol{u}_h, \boldsymbol{v}_h) := \nu \int_{\Omega_h^n} \nabla \boldsymbol{u} : \nabla \boldsymbol{v} \, \mathrm{d}\boldsymbol{x} + \nu N_h^n(\boldsymbol{u}_h, \boldsymbol{v}_h),$$

$$N_h^n(\boldsymbol{u}_h, \boldsymbol{v}_h) := N_{h,c}^n(\boldsymbol{u}_h, \boldsymbol{v}_h) + N_{h,c}^n(\boldsymbol{v}_h, \boldsymbol{u}_h) + N_{h,s}^n(\boldsymbol{u}_h, \boldsymbol{v}_h),$$

where

$$N_{h,c}^n(\boldsymbol{u}_h, \boldsymbol{v}_h) := \int_{\Gamma_h^n} (-\partial_{\boldsymbol{n}} \boldsymbol{u}_h) \cdot \boldsymbol{v}_h \, \mathrm{d}s \quad \text{and} \quad N_{h,s}^n(\boldsymbol{u}_h, \boldsymbol{v}_h) := \int_{\Gamma_h^n} \frac{\sigma}{h} \boldsymbol{u}_h \cdot \boldsymbol{v}_h \, \mathrm{d}s$$

are the consistency (symmetry) and penalty terms of Nitsche's method while $\sigma > 0$ is the penalty parameter, and $\partial_{\boldsymbol{n}}$ denotes the normal derivative. The velocity–pressure coupling term is given by

$$b_h^n(\boldsymbol{v}, q) = -\int_{\Omega_h^n} q \nabla \cdot \boldsymbol{v} \, \mathrm{d}\boldsymbol{x} + \int_{\Gamma_h^n} p \boldsymbol{v} \cdot \boldsymbol{n} \, \mathrm{d}s.$$

In order to realize the discrete extension of the velocity and to stabilize the method with respect to essentially arbitrary mesh-interface cut positions we use ghost-penalty stabilization. This term is given by

$$s_h^n((\boldsymbol{u}_h^n, p_h^n), (\boldsymbol{v}_h, q_h)) = \gamma_{s,u} \nu i_h^n(\boldsymbol{u}_h^n, \boldsymbol{v}_h) + \gamma_{s,u}' \frac{1}{\nu} i_h^n(\boldsymbol{u}_h^n, \boldsymbol{v}_h) - \gamma_{s,p} \frac{1}{\nu} j_h^n(p_h^n, q_h)$$

with stabilization parameters $\gamma_{s,u}, \gamma_{s,u}', \gamma_{s,p} > 0$. A suitable choice for these parameters will be discussed later, cf. Remark 5.7 below. The velocity ghost-penalty operator $i_h^n(\cdot, \cdot)$ stabilizes the velocity w.r.t. arbitrary bad cut configurations and implicitly defines an extension of the velocity field. It will therefore act on a strip of elements both inside and outside the physical domain, in order for us to have control over the velocity on the entire active domain $\mathcal{T}_{h,\delta_h}^n$. The pressure ghost-penalty operator stabilizes the pressure in the $\mathcal{L}^2$-norm, and is needed to give an inf-sup property for unfitted finite elements (Guzmán & Olshanskii, 2017). This operator will therefore only act in the direct vicinity of the domain boundary and only on elements that have at least some part in the physical domain.

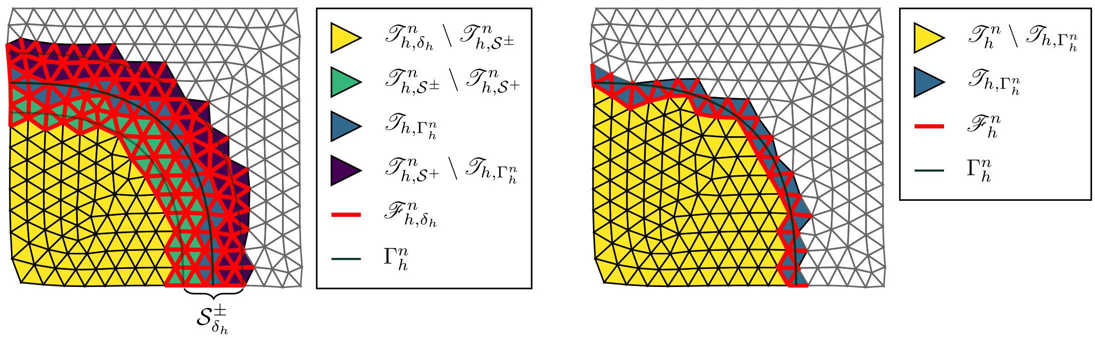

(a) Active velocity elements **(b)** Active pressure elements

FIG. 1. The different stability and extension elements for both the velocity and pressure. Note that the interior (yellow) elements that have a red facet are also used by the direct ghost penalty operator.

4.1.1 *The ghost-penalty operator.* The stabilization bilinear form $s_h(\cdot,\cdot)$ has two purposes here. First, it stabilizes the discrete problem (4.1) with respect to domain boundary-mesh cut position and it implicitly provides the extension of the velocity field that is needed to allow the method of lines approach. To the best of our knowledge there are currently three different versions of the ghost-penalty stabilization operator. A *local projection stabilization (LPS)-type-type* version was the first ghost-penalty operator, proposed in Burman (2010). The *normal derivative jump* version is probably the most widely used variant, see e.g., Burman & Hansbo (2012), Burman *et al.* (2014), Gürkan & Massing (2019), Massing *et al.* (2014), Schott & Wall (2014). We will use the *direct version* of the ghost penalty operator introduced in Preuß (2018). For details on all three ghost penalty operators see Lehrenfeld & Olshanskii (2019). We will only provide details on the direct version used here. However, the other versions of the ghost-penalty operator could also be used instead.

For the velocity ghost-penalty operator we define the set of elements in the boundary strip

$$\mathscr{T}^n_{h,\mathcal{S}^\pm} := \{K \in \widetilde{\mathscr{T}}_h \mid \exists \boldsymbol{x} \in K \text{ with } \operatorname{dist}(\boldsymbol{x}, \varGamma^n_h) \leq \delta_h\}$$

and the set of interior facets in this strip

$$\mathscr{F}^n_{h,\delta_h} := \{F = \overline{T}_1 \cap \overline{T}_2 \mid T_1 \in \mathscr{T}^n_{h,\delta_h}, T_2 \in \mathscr{T}^n_{h,\mathcal{S}^\pm}, T_1 \neq T_2 \text{ and } \operatorname{meas}_{d-1}(F) > 0\}.$$

Furthermore, for the pressure ghost-penalty operator, we define the set of *boundary elements*

$$\mathscr{T}_{h,\varGamma^n_h} := \{K \in \mathscr{T}^n_h \mid \exists \boldsymbol{x} \in K \text{ with } \boldsymbol{x} \in \varGamma^n_h\},$$

and the set of interior facets of these elements

$$\mathscr{F}^n_h := \{F = \overline{T}_1 \cap \overline{T}_2 \mid T_1 \in \mathscr{T}^n_h, T_2 \in \mathscr{T}_{h,\varGamma^n_h}, T_1 \neq T_2 \text{ and } \operatorname{meas}_{d-1}(F) > 0\}.$$

A sketch of the different sets of element and facets for both the velocity, and pressure can be seen in Fig. 1.

To define the stabilization operator we require some further notation. For a facet in the extension strip $\mathscr{F}^n_{h,\delta_h} \ni F = \overline{T}_1 \cap \overline{T}_2$ let $\omega_F = T_1 \cup T_2$ be the corresponding *facet patch*. We then consider $[\![u]\!] := u_1 - u_2$ with $u_i = \mathcal{E}^{\mathbb{P}} u\big|_{T_i}$, where $\mathcal{E}^{\mathbb{P}} : \mathbb{P}^m(K) \to \mathbb{P}^m(\mathbb{R}^d)$ is the canonical extension of a polynomial to $\mathbb{R}^d$.

The velocity ghost-penalty operator is then defined as

$$i^n_h(\boldsymbol{u}_h, \boldsymbol{v}_h) = \sum_{F \in \mathscr{F}^n_{h,\delta_h}} \frac{1}{h^2} \int_{\omega_F} [\![\boldsymbol{u}_h]\!] \cdot [\![\boldsymbol{v}_h]\!] \mathrm{d}\boldsymbol{x}$$

and the pressure ghost-penalty operator is defined as

$$j^n_h((p_h, q_h)) = \sum_{F \in \mathscr{F}^n_h} \int_{\omega_F} [\![p_h]\!] \cdot [\![q_h]\!] \mathrm{d}\boldsymbol{x}.$$

For the analysis we will also need to insert general $\mathcal{L}^2$-functions as arguments of the ghost-penalty operators. In this case we take $u_i = \mathcal{E}^{\mathbb{P}} \Pi_{T_i} u\big|_{T_i}$, where Π_{T_i} is the $\mathcal{L}^2(T_i)$-projection onto $\mathbb{P}^m(T_i)$.

From Lehrenfeld & Olshanskii (2019, Lemma 5.8) we have a consistency result for the diffusion ghost-penalty operator. The same result for $j^n_h(\cdot,\cdot)$ follows by a repetition of the same arguments and taking the h-scaling into account.

Lemma 4.1 (Consistency). Let $\boldsymbol{w} \in \boldsymbol{\mathcal{H}}^{m+1}(\mathcal{O}^n_{\delta_h,\mathscr{T}})$ and $r \in \mathcal{H}^m(\mathcal{O}^n_{\mathscr{T}})$, $n = 1, \dots, N$, $m \geq 1$. Then it holds that

$$i^n_h(\boldsymbol{w}, \boldsymbol{w}) \leq ch^{2m} \|\boldsymbol{w}\|^2_{\boldsymbol{\mathcal{H}}^{m+1}(\mathcal{O}^n_{\delta_h,\mathscr{T}})}$$
$$j^n_h(r, r) \leq ch^{2m} \|r\|^2_{\mathcal{H}^m(\mathcal{O}^n_{\mathscr{T}})}.$$

Furthermore, let $\mathcal{I}^*$ be the Scott–Zhang interpolation operator (Scott & Zhang, 1990) for the velocity and for the pressure space. Then we also have

$$i^n_h(\boldsymbol{w} - \mathcal{I}^*\boldsymbol{w}, \boldsymbol{w} - \mathcal{I}^*\boldsymbol{w}) \leq ch^{2m} \|\boldsymbol{w}\|^2_{\boldsymbol{\mathcal{H}}^{m+1}(\mathcal{O}^n_{\delta_h,\mathscr{T}})}$$
$$j^n_h(r - \mathcal{I}^* r, r - \mathcal{I}^* r) \leq ch^{2m} \|r\|^2_{\mathcal{H}^m(\mathcal{O}^n_{\delta_h,\mathscr{T}})}.$$

5. Analysis of the method

The analysis of the fully discrete method in this section is structured as follows. In Section 5.1 we will introduce further notation, concepts and basic necessary results from the literature needed for the analysis. Section 5.2 will then cover the existence and uniqueness of the solution to the fully discretized system. The stability of this solution is then discussed in Section 5.3. We then cover some technical details on the geometry approximation made by integrating over discrete approximations Ω^n_h of the exact domain Ω^n in Section 5.4. With the tools covered in these sections we then show the consistency of the method in both time and space in Section 5.5. With this consistency result we are then able to prove an error estimate for the solution in the energy norm in Section 5.6.

5.1 *Preliminaries*

For the analysis we require some further notation and definitions. We define the *extension strip mesh* as

$$\mathscr{T}^n_{h,\mathcal{S}^+} := \{K \in \widetilde{\mathscr{T}}_h \mid \exists \boldsymbol{x} \in \widetilde{\Omega} \setminus \Omega^n_h \text{ with } \operatorname{dist}(\boldsymbol{x}, \Gamma^n_h) \le \delta_h\}.$$

We also define the *sharp strips* as

$$\mathcal{S}^{\pm}_{\delta_h}(\Omega^n_h) := \{\boldsymbol{x} \in \widetilde{\Omega} \mid \operatorname{dist}(\boldsymbol{x}, \Gamma^n_h) \le \delta_h\} \quad \text{and} \quad \mathcal{S}^{+}_{\delta_h}(\Omega^n_h) := \{\boldsymbol{x} \in \widetilde{\Omega} \setminus \Omega^n_h \mid \operatorname{dist}(\boldsymbol{x}, \Gamma^n_h) \le \delta_h\}.$$

Furthermore, we define the *discrete extended domain* $\mathcal{O}_{\delta_h}(\Omega^n_h) := \mathcal{S}^{\pm}_{\delta_h}(\Omega^n_h) \cup \Omega^n_h$. In the analysis we require that δ is sufficiently large, such that

$$\mathcal{O}^n_{\delta_h,\mathscr{T}} \subset \mathcal{O}_\delta(\Omega^n) \quad \text{and} \quad \Omega^n_h \subset \mathcal{O}_\delta(\Omega(t)),\ t \in I_n = [t_{n-1}, t_n), \tag{5.1}$$

for $n = 1, \dots, N$. Furthermore, for ease and brevity of notation, we write $a \lesssim b$ if it holds that $a \le cb$ with a constant $c > 0$ independent of the mesh size h, the time step Δt, the time t and the mesh-interface cut position. Similarly, we write $a \simeq b$ if both $a \lesssim b$ and $b \lesssim a$ holds.

For the analysis we shall consider the following mesh dependent norms. For the velocity we take

$$|||\boldsymbol{v}|||^2_n := \|\nabla \boldsymbol{v}\|^2_{\Omega^n_h} + \|h^{-1/2}\boldsymbol{v}\|^2_{\Gamma^n_h} + \|h^{1/2}\partial_{\boldsymbol{n}}\boldsymbol{v}\|^2_{\Gamma^n_h}$$

$$|||\boldsymbol{v}|||^2_{*,n} := \|\nabla \boldsymbol{v}\|^2_{\mathcal{O}^n_{\delta_h,\mathscr{T}}} + \|h^{-1/2}\boldsymbol{v}\|^2_{\Gamma^n_h}, \qquad \|\boldsymbol{v}\|_{-1,n} := \sup_{\boldsymbol{w}\in \boldsymbol{V}^n_h} \frac{(\boldsymbol{v}, \boldsymbol{w})_{\Omega^n_h}}{|||\boldsymbol{w}|||_{*,n}}.$$

For the pressure we introduce

$$|||q|||^2_n := \|q\|^2_{\Omega^n_h} + \|h^{1/2}q\|^2_{\Gamma^n_h}, \qquad |||q|||_{*,n} := \|q\|_{\mathcal{O}^n_{\mathscr{T}}}$$

and for the product space

$$|||(\boldsymbol{u}, p)|||^2_{*,n} := |||\boldsymbol{u}|||^2_{*,n} + |||p|||^2_{*,n}.$$

Note that $|||\cdot|||_n$-norms are defined on the physical domain and add control on the normal derivative of the velocity and the trace of the pressure at the boundary. These norms arise naturally to bound the bilinear form $a^n_h(\boldsymbol{u}, \boldsymbol{v})$ for functions $\boldsymbol{u}, \boldsymbol{v} \in \boldsymbol{\mathcal{H}}^1(\Omega^n_h)$. The second type of norms, the $|||\cdot|||_{*,n}$-norms, are defined on the entire active domain and therefore represent proper norms for discrete finite element functions.

5.1.1 *Basic estimates.*

For $v_h \in \mathbb{P}^k(K),\ K \in \widetilde{\mathscr{T}}_h$ we have the inverse and trace estimates:

$$\|\nabla v_h\|_K \lesssim h_K^{-1}\|v_h\|_K, \tag{5.2a}$$

$$\|h^{1/2}\partial_{\boldsymbol{n}} v_h\|_F \lesssim \|\nabla v_h\|_K, \tag{5.2b}$$

$$\|h^{1/2}\partial_{\boldsymbol{n}} v_h\|_{K\cap\Gamma^n_h} \lesssim \|\nabla v_h\|_K. \tag{5.2c}$$

For (5.2a) and (5.2b) see for example Quarteroni (2014). For a proof of (5.2c) see Hansbo & Hansbo (2002). For $v \in \mathcal{H}^1(K),\ K \in \mathscr{T}^n_{h,\delta_h}$ we also have the following trace inequality from Hansbo & Hansbo (2002)

$$\|v\|_{K\cap\Gamma_h^n} \lesssim h_K^{-1/2}\|v\|_K + h_K^{1/2}\|\nabla v\|_K. \tag{5.3}$$

It follows from these estimates that

$$|||\boldsymbol{v}_h|||_n \lesssim |||\boldsymbol{v}_h|||_{*,n} \quad \text{and} \quad |||q_h|||_n \lesssim |||q_h|||_{*,n} \tag{5.4}$$

for all $\boldsymbol{v}_h \in \boldsymbol{V}_h^n$ and $q_h \in Q_h^n$. Furthermore, we have a discrete version of the Poincaré inequality

$$\|\boldsymbol{v}_h\|_{\mathcal{O}^n_{\delta_h,\mathscr{T}}} \le c_{P,h}|||\boldsymbol{v}_h|||_{*,n} \tag{5.5}$$

for all $\boldsymbol{v}_h \in \boldsymbol{V}_h$, see (Massing *et al.*, 2014, Lemma 7.2) for a proof thereof.

5.1.2 *Interpolation properties.* From Apel (1999), Scott & Zhang (1990) we take the following standard interpolation result.

LEMMA 5.1 Let $K \in \widetilde{\mathscr{T}}_h$ and $w \in \mathcal{H}^m(K)$, $m \ge 1$. Then it holds for the Scott–Zhang interpolant

$$\|D^k(w - \mathcal{I}^* w)\|_K \le h^{m-k}\|D^m w\|_K, \qquad 0 \le k \le m,$$

and on the boundary of an element

$$\|w - \mathcal{I}^* w\|_{\partial K} \le h^{m-1/2}\|D^m w\|_K.$$

LEMMA 5.2 Let $\boldsymbol{v} \in \boldsymbol{\mathcal{H}}^{m+1}(\Omega^n)$ and $q \in \mathcal{H}^m(\Omega^n)$, $m \ge 1$. Then it holds that

$$|||\mathcal{E}\boldsymbol{v} - \mathcal{I}^*\mathcal{E}\boldsymbol{v}|||_n \lesssim h^m\|\boldsymbol{v}\|_{\boldsymbol{\mathcal{H}}^{m+1}(\Omega^n)} \tag{5.6a}$$

$$|||\mathcal{E}q - \mathcal{I}^*\mathcal{E}q|||_n \lesssim h^m\|q\|_{\mathcal{H}^m(\Omega^n)}. \tag{5.6b}$$

Proof. See also Massing *et al.* (2014, Lemma 4.1). For (5.6a) we consider the volume and boundary contribution to the $|||\cdot|||_n$-norm separately. Let $\boldsymbol{w} = \mathcal{E}\boldsymbol{v}$.

We split the volume terms into element contributions. On interior elements we simply apply Lemma 5.1. For cut simplices we extend the norm onto the entire element before applying the interpolation estimate. Summing up over all active elements and applying (3.3a) in combination with (5.1) gives

$$\|\nabla(\boldsymbol{w} - \mathcal{I}^*\boldsymbol{w})\|_{\Omega_h^n} \lesssim h^m\|\boldsymbol{w}\|_{\boldsymbol{\mathcal{H}}^{m+1}(\mathcal{O}^n_{\delta_h,\mathscr{T}})} \lesssim h^m\|\boldsymbol{v}\|_{\boldsymbol{\mathcal{H}}^m(\Omega^n)}.$$

Similarly, on each cut element, we can estimate the boundary terms using (5.3) and apply the interpolation estimate:

$$\|h^{1/2}\partial_{\boldsymbol{n}}(\boldsymbol{w}-\mathcal{I}^*\boldsymbol{w})\|_{K\cap\Gamma_h^n} \lesssim \|\nabla(\boldsymbol{w}-\mathcal{I}^*\boldsymbol{w})\|_K + h\|\nabla^2(\boldsymbol{w}-\mathcal{I}^*\boldsymbol{w})\|_K \lesssim h^m\|\boldsymbol{w}\|_{\boldsymbol{\mathcal{H}}^{m+1}(K)}$$

and

$$\|h^{-1/2}(\boldsymbol{w}-\mathcal{I}^*\boldsymbol{w})\|_{K\cap\Gamma_h^n} \lesssim h^{-1}\|\boldsymbol{w}-\mathcal{I}^*\boldsymbol{w}\|_K + \|\nabla(\boldsymbol{w}-\mathcal{I}^*\boldsymbol{w})\|_K \lesssim h^m\|\boldsymbol{w}\|_{\boldsymbol{\mathcal{H}}^{m+1}(K)}.$$

Summing up over all cut elements and again applying (3.3a) in combination with (5.1) then proves (5.6a). □

5.1.3 *The ghost-penalty mechanism.* We assume that for every strip element $K \in \mathscr{T}^n_{h,\mathcal{S}^+}$ there exists an uncut element $K' \in \mathscr{T}^n_{h,\delta_h} \setminus \mathscr{T}^n_{h,\mathcal{S}^+}$, which can be reached by a path that crosses a bounded number of facets $F \in \mathscr{F}^n_h$. We assume that the number of facets that have to be crossed to reach K' from K is bounded by a constant $L \lesssim (1+\frac{\delta_h}{h})$ and that every uncut element $K' \in \mathscr{T}^n_{h,\delta_h} \setminus \mathscr{T}^n_{h,\mathcal{S}^+}$ is the end of at most M such paths with M bounded independent of Δt and h. In other words, each uncut elements 'supports' at most M strip elements. See Lehrenfeld & Olshanskii (2019, Remark 5.4) for a justification as to why the above assumption is reasonable if the mesh resolves the domain boundary sufficiently well.

LEMMA 5.3 For all $\boldsymbol{v}_h \in \boldsymbol{V}^n_h$ and $q_h \in Q^n_h$ it holds that

$$\|\nabla\boldsymbol{v}_h\|^2_{\mathcal{O}^n_{\delta_h,\mathscr{T}}} \simeq \|\nabla\boldsymbol{v}_h\|^2_{\Omega^n_h} + L\cdot i^n_h(\boldsymbol{v}_h,\boldsymbol{v}_h) \tag{5.7a}$$

$$\|\boldsymbol{v}_h\|^2_{\mathcal{O}^n_{\delta_h,\mathscr{T}}} \simeq \|\boldsymbol{v}_h\|^2_{\Omega^n_h} + h^2L\cdot i^n_h(\boldsymbol{v}_h,\boldsymbol{v}_h) \tag{5.7b}$$

$$\|q_h\|^2_{\mathcal{O}^n_{\mathscr{T}}} \simeq \|q_h\|^2_{\Omega^n_h} + j^n_h(q_h,q_h). \tag{5.7c}$$

Proof. For the first inequality in both (5.7a) and (5.7c) we refer to Lehrenfeld & Olshanskii (2019, Lemma 5.5). For the second bound we use the fact that we can bound the direct version of the ghost penalty operator by the normal derivative jump version, see (Preuß, 2018, Chapter 3, Remark 6). The upper bound then follows by an application of the inverse (trace) estimates (5.2a) and (5.2b), see (Massing *et al.*, 2014, Proposition 5.1). □

5.2 *Unique solvability*

For the stabilized diffusion and pressure-coupling bilinear forms we collect the following continuity result from Burman & Hansbo (2012, Lemma 7) and Massing *et al.* (2014, Proposition 5.2), respectively, with $\nu = 1$ and $L = 1$. For general ν and L the proof is a repetition of the same arguments while taking the larger ghost-penalty region into account.

LEMMA 5.4 (Continuity). For the diffusion bilinear form we have for all $\boldsymbol{v},\boldsymbol{w} \in \boldsymbol{\mathcal{H}}^1(\mathcal{O}_\delta(\Omega^n))$ that it holds

$$a^n_h(\boldsymbol{v},\boldsymbol{w}) \lesssim \nu|||\boldsymbol{v}|||_n|||\boldsymbol{w}|||_n \tag{5.8}$$

and for all $\boldsymbol{v}_h, \boldsymbol{w}_h \in \boldsymbol{V}_h^n$ it holds that

$$a_h^n(\boldsymbol{v}_h, \boldsymbol{w}_h) + \nu L i_h^n(\boldsymbol{v}_h, \boldsymbol{w}_h) \lesssim \nu |||\boldsymbol{v}_h|||_{*,n} |||\boldsymbol{w}_h|||_{*,n}. \tag{5.9}$$

Furthermore, for the velocity–pressure coupling bilinear form, we have for all $q \in \mathcal{L}^2(\mathcal{O}_\delta(\Omega^n))$ and $\boldsymbol{v} \in \boldsymbol{\mathcal{H}}^1(\mathcal{O}_\delta(\Omega^n))$ that

$$b_h^n(q, \boldsymbol{v}) \lesssim |||q|||_n |||\boldsymbol{v}|||_n$$

and for all $q_h \in Q_h^n$ and $\boldsymbol{v}_h \in \boldsymbol{V}_h^n$ that

$$b_h^n(q_h, \boldsymbol{v}_h) \lesssim |||q_h|||_{*,n} |||\boldsymbol{v}_h|||_{*,n}.$$

We further take the following coercivity result from the literature. The proof for $\nu = 1$ and $L = 1$ can be found in Burman & Hansbo (2012, Lemma 6) or Burman & Hansbo (2014, Lemma 4.2). The proof for general $\nu > 0$ and $L > 1$ is again a repetition of the identical arguments and taking the ghost-penalty strip width into account.

Lemma 5.5 (Coercivity). There exists a constant $c_{L5.5} > 0$, independent of h and the mesh-interface cut position, such that for sufficiently large $\sigma > 0$ there holds

$$a_h^n(\boldsymbol{u}_h, \boldsymbol{u}_h) + \nu L i_h^n(\boldsymbol{u}_h, \boldsymbol{v}_h) \geq \nu c_{L5.5} |||\boldsymbol{u}_h|||_{*,n}^2$$

for all $\boldsymbol{u}_h \in \boldsymbol{V}_h$.

As a consequence of Lemma 5.4 and Lemma 5.5 we have the following result. A proof may be found in Guzmán & Olshanskii (2017, Corollary 1).

Lemma 5.6 Let $\Omega_{h,i}^n := \Omega_h^n \setminus \{\boldsymbol{x} \in K \mid K \in \mathscr{T}_{h,\Gamma_h^n}\}$ denote the interior, uncut domain. It then holds for all $q_h \in Q_h^n$ with $q_h\big|_{\Omega_{h,i}^n} \in \mathcal{L}_0^2(\Omega_{h,i}^n)$ that

$$\beta \|q_h\|_{\Omega_h^n} \leq \sup_{\boldsymbol{v}_h \in \boldsymbol{V}_h^n} \frac{b_h(q_h, \boldsymbol{v}_h)}{|||\boldsymbol{v}_h|||_{*,n}} + j_h^n(q_h, q_h)^{1/2}. \tag{5.10}$$

The constant $\beta > 0$ is independent of h and q_h.

Remark 5.7 (Choice of ghost-penalty parameter). From Lemma 5.4 and Lemma 5.5 we see that the velocity ghost-penalty parameter should scale with the strip-width L. This is necessary, in order for an exterior unphysical, but active element, to obtain support from an uncut interior element for which we have to cross at most L elements to reach it, cf. Assumption A2. As this first part of the ghost-penalties is related to the stabilization of the viscosity bilinear form $a_h^n(\cdot,\cdot)$ only it has a scaling with ν. We require the same mechanism also for the implicit extension of functions. As we will see in the analysis below this requires the same ghost-penalty, however with the different scaling $1/\nu$.

The pressure ghost-penalty operator in Lemma 5.6 does not need a scaling with L, as we require these ghost-penalties only for stabilizing the velocity-pressure coupling, but not for the extension of the pressure field into a δ-neighbourhood.

For simplicity of the analysis we choose a common ghost-penalty stabilization parameter γ_s, which we use to set $\gamma_{s,u} = \gamma'_{s,u} = L\gamma_s$ and $\gamma_{s,p} = \gamma_s$.

We now collect all fully implicit nonghost-penalty terms in the bilinear form

$$A_h^n((\boldsymbol{u}_h^n, p_h^n), (\boldsymbol{v}_h, q_h)) := \frac{1}{\Delta t}(\boldsymbol{u}_h^n, \boldsymbol{v}_h)_{\Omega_h^n} + a_h^n(\boldsymbol{u}_h^n, \boldsymbol{v}_h) + b_h^n(p_h^n, \boldsymbol{v}_h) + b_h^n(q_h, \boldsymbol{u}_h^n)$$

and the explicit terms in the linear form

$$F_h^n(\boldsymbol{v}_h) := \frac{1}{\Delta t}(\boldsymbol{u}_h^{n-1}, \boldsymbol{v}_h)_{\Omega_h^n} + \boldsymbol{f}_h^n(\boldsymbol{v}_h).$$

We can then rewrite problem (4.1) as: find $(\boldsymbol{u}_h^n, p_h^n) \in \boldsymbol{V}_h^n \times Q_h^n$, such that

$$A_h^n((\boldsymbol{u}_h^n, p_h^n), (\boldsymbol{v}_h, q_h)) + s_h^n((\boldsymbol{u}_h^n, p_h^n), (\boldsymbol{v}_h, q_h)) = F_h^n(\boldsymbol{v}_h^n) \tag{5.11}$$

for all $(\boldsymbol{v}_h, q_h) \in \boldsymbol{V}_h^n \times Q_h^n$. This problem is indeed well posed:

THEOREM 5.8 (Well posedness). Consider the norm $|||(\boldsymbol{u}_h^n, p_h^n)|||_{\flat,n}^2 := \frac{1}{\Delta t}\|\boldsymbol{u}_h^n\|_{\Omega_h^n}^2 + |||(\boldsymbol{u}_h^n, p_h^n)|||_{*,n}^2$. There exists a constant $c_{T5.8} > 0$ such that for all $(\boldsymbol{u}_h^n, p_h^n) \in \boldsymbol{V}_h^n \times Q_h^n$ it holds that

$$\sup_{(\boldsymbol{v}_h, q_h) \in \boldsymbol{V}_h^n \times Q_h^n} \frac{A_h^n((\boldsymbol{u}_h^n, p_h^n), (\boldsymbol{v}_h, q_h)) + s_h^n((\boldsymbol{u}_h^n, p_h^n), (\boldsymbol{v}_h, q_h))}{|||(\boldsymbol{v}_h, q_h)|||_{\flat,n}} \geq c_{T5.8} |||(\boldsymbol{u}_h^n, p_h^n)|||_{\flat,n}. \tag{5.12}$$

The solution $(\boldsymbol{u}_h^n, p_h^n) \in \boldsymbol{V}_h^n \times Q_h^n$ to (5.11) exists and is unique.

Proof. The proof follows the same lines as for the unfitted Stokes problem using CutFEM in Massing *et al.* (2014), Guzmán & Olshanskii (2017). Let $(\boldsymbol{u}_h^n, p_h^n) \in \boldsymbol{V}_h^n \times Q_h^n$ be given and let $\boldsymbol{w}_h \in \boldsymbol{V}_h^n$ be the test function, such that (5.10) holds and w.l.o.g. that $|||\boldsymbol{w}_h|||_{*,n} = \|p_h^n\|_{\Omega_h^n}$. Testing (5.11) with $(-\boldsymbol{w}_h, 0)$ and using Cauchy–Schwarz, Lemma 5.4, Lemma 5.6 and the weighted Young's inequality then gives

$$\begin{aligned}
(A_h^n + s_h^n)((\boldsymbol{u}_h^n, p_h^n), (-\boldsymbol{w}_h, 0)) &= -\frac{1}{\Delta t}(\boldsymbol{u}_h^n, \boldsymbol{w}_h)_{\Omega_h^n} - \left(a_h^n + (\nu + 1/\nu i_h^n)\right)(\boldsymbol{u}_h^n, \boldsymbol{w}_h) + b_h^n(-p_h^n, \boldsymbol{w}_h) \\
&\geq -\frac{1}{\Delta t}\|\boldsymbol{u}_h^n\|_{\Omega_h^n}\|\boldsymbol{w}_h\|_{\Omega_h^n} - c|||\boldsymbol{u}_h^n|||_{*,n}|||\boldsymbol{w}_h|||_{*,n} + \beta\|p_h^n\|_{\Omega_h^n}|||\boldsymbol{w}_h|||_{*,n} \\
&\qquad - j_h^n(p_h^n, p_h^n)^{1/2}|||\boldsymbol{w}_h|||_{*,n} \\
&\geq -\frac{1}{2\varepsilon_1 \Delta t^2}\|\boldsymbol{u}_h^n\|_{\Omega_h^n}^2 - \frac{c}{2\varepsilon_2}|||\boldsymbol{u}_h^n|||_{*,n}^2 - \frac{1}{2\varepsilon_3} j_h^n(p_h^n, p_h^n) \\
&\qquad + \left(\beta - \frac{\varepsilon_1}{2} - \frac{c_1\varepsilon_2}{2} - \frac{\varepsilon_3}{2}\right)\|p_h^n\|_{\Omega_h^n}^2.
\end{aligned}$$

Choosing $\varepsilon_1, \varepsilon_2, \varepsilon_3 > 0$ such that $(\beta - \varepsilon_1/2 - c\varepsilon_2/2 - \varepsilon_3/2) > 0$ we then have

$$(A_h^n + s_h^n)((\boldsymbol{u}_h^n, p_h^n), (-\boldsymbol{w}_h, 0)) \geq -\frac{c_1}{\Delta t^2}\|\boldsymbol{u}_h^n\|_{\Omega_h^n}^2 - c_2|||\boldsymbol{u}_h^n|||_{*,n}^2 + c_3\|p_h^n\|_{\Omega_h^n}^2 - c_4 j_h^n(p_h^n, p_h^n).$$

Furthermore, with the test function $(\boldsymbol{v}_h, q_h) = (\boldsymbol{u}_h^n, -p_h^n)$ in (5.11) and using Lemma 5.5, we have

$$(A_h^n + s_h^n)((\boldsymbol{u}_h^n, p_h^n), (\boldsymbol{u}_h^n, -p_h^n)) \geq \frac{1}{\Delta t}\|\boldsymbol{u}_h^n\|^2_{\Omega_h^n} + c_{L5.5}|||\boldsymbol{u}_h^n|||^2_{*,n} + j_h^n(p_h^n, p_h^n).$$

Combining these two estimates we have with a suitable choice of $\delta > 0$ that

$$(A_h^n + s_h^n)((\boldsymbol{u}_h^n, p_h^n), (\boldsymbol{u}_h^n - \Delta t\delta \boldsymbol{w}_h, -p_h^n)) \geq c|||(\boldsymbol{u}_h^n, p_h^n)|||^2_{\flat,n}.$$

Since $|||(\boldsymbol{u}_h^n - \Delta t\delta\boldsymbol{w}_h, -p_h^n)|||_{\flat,n} \leq (1 + \Delta t\delta)|||(\boldsymbol{u}_h^n, p_h^n)|||_{\flat,n}$ we then have (5.12).

The continuity of $(A_h^n + s_h^n)$ in the $|||(\cdot,\cdot)|||_{\flat,n}$-norm can be easily shown. The existence and uniqueness of the solution then follow by the Banach–Nečas–Babuška Theorem (see e.g., Ern & Guermond, 2004, Theorem 2.6). $\square$

5.3 *Stability*

For the fully discrete method we have a discrete counterpart of Lemma 3.2.

THEOREM 5.9 For the velocity solution $\boldsymbol{u}_h^k \in \boldsymbol{V}_h^n$, $k = 1, \ldots, N$ of (4.1) we have the stability estimate

$$\begin{aligned}
&\|\boldsymbol{u}_h^k\|^2_{\Omega_n^k} + \Delta t \sum_{n=1}^{k}\Big[\frac{\nu c_{T5.9\text{a}}}{2}|||\boldsymbol{u}_h^n|||^2_{*,n} + \frac{L}{\nu} i_h^n(\boldsymbol{u}_h^n, \boldsymbol{u}_h^n)\Big] \\
&\quad \leq \exp(c_{T5.9\text{b}}\nu^{-1}t_k)\left[\|\boldsymbol{u}_h^0\|^2_{\Omega_n^0} + \frac{\nu\Delta t c_{T5.9\text{a}}}{2}|||\boldsymbol{u}_h^0|||^2_{*,0} + \frac{L}{\nu} i_h^0(\boldsymbol{u}_h^0, \boldsymbol{u}_h^0) + \Delta t\sum_{n=1}^{k}\frac{c_{P,h}^2}{\nu c_{T5.9\text{a}}}\|\boldsymbol{f}_h^n\|^2_{\Omega_h^n}\right].
\end{aligned}$$

Proof. Testing (4.1) with $(\boldsymbol{v}_h, q_h) = 2\Delta t(\boldsymbol{u}_h^n, -p_h^n) \in \boldsymbol{V}_h^n \times Q_h^n$ and using the identity

$$2(\boldsymbol{u}^n - \mathcal{E}\boldsymbol{u}^{n-1}, \boldsymbol{u}^n)_{\Omega^n} = \|\boldsymbol{u}^n\|^2_{\Omega^n} + \|\boldsymbol{u}^n - \mathcal{E}\boldsymbol{u}^{n-1}\|^2_{\Omega^n} - \|\mathcal{E}\boldsymbol{u}^{n-1}\|^2_{\Omega^n} \tag{5.13}$$

gives us

$$\begin{aligned}
\|\boldsymbol{u}_h^n\|^2_{\Omega_h^n} + \|\boldsymbol{u}_h^n - \boldsymbol{u}_h^{n-1}\|^2_{\Omega_h^n} + 2\Delta t\Big[a_h^n(\boldsymbol{u}_h^n, \boldsymbol{u}_h^n) + \nu\gamma_s i_h^n(\boldsymbol{u}_h^n, \boldsymbol{u}_h^n) + \frac{\gamma_s}{\nu} i_h^n(\boldsymbol{u}_h^n, \boldsymbol{u}_h^n) + \frac{\gamma_s}{\nu} j_h^n(p_h^n, p_h^n)\Big]& \\
= 2\Delta t\boldsymbol{f}_h^n(\boldsymbol{u}_h^n) + \|\boldsymbol{u}_h^{n-1}\|^2_{\Omega_h^n}&.
\end{aligned}$$

Using the coercivity result from Lemma 5.5 and the fact that $\|\boldsymbol{u}_h^n - \boldsymbol{u}_h^{n-1}\|^2_{\Omega_h^n} + \frac{2\Delta t\gamma_s}{\nu} j_h^n(p_h^n, p_h^n) \geq 0$ we get

$$\|\boldsymbol{u}_h^n\|^2_{\Omega_h^n} + 2\Delta t\nu c_{L5.5}|||\boldsymbol{u}_h^n|||^2_{*,n} + \Delta t\frac{2}{\nu} L i_h^n(\boldsymbol{u}_h^n, \boldsymbol{u}_h^n) \leq 2\Delta t\boldsymbol{f}_h^n(\boldsymbol{u}_h^n) + \|\boldsymbol{u}_h^{n-1}\|^2_{\Omega_h^n}. \tag{5.14}$$

To bound the forcing term we use the Cauchy–Schwarz inequality, the discrete Poincaré inequality (5.5) as well as the weighted Young's inequality, which gives

$$f_h^n(\boldsymbol{u}_h^n) \le \|\boldsymbol{f}_h^n\|_{\Omega_h^n}\|\boldsymbol{u}_h^n\|_{\Omega_h^n} \le \|\boldsymbol{f}_h^n\|_{\Omega_h^n} c_{P,h} |||\boldsymbol{u}_h^n|||_{*,n} \le \frac{c_{P,h}^2\|\boldsymbol{f}_h^n\|_{\Omega_h^n}^2}{2\varepsilon} + \frac{\varepsilon|||\boldsymbol{u}_h^n|||_{*,n}^2}{2}.$$

Inserting this into (5.14) with the choice $\varepsilon = \nu c_{L5.5}$ then gives

$$\|\boldsymbol{u}_h^n\|_{\Omega_h^n}^2 + \Delta t \nu c_{L5.5}|||\boldsymbol{u}_h^n|||_{*,n}^2 + \Delta t\frac{2}{\nu}Li_h^n(\boldsymbol{u}_h^n,\boldsymbol{u}_h^n) \le \frac{c_{P,h}^2\Delta t}{\nu c_{L5.5}}\|\boldsymbol{f}_h^n\|_{\Omega_h^n}^2 + \|\boldsymbol{u}_h^{n-1}\|_{\Omega_h^n}^2. \tag{5.15}$$

To obtain a bound on $\|\boldsymbol{u}_h^{n-1}\|_{\Omega_h^n}^2$ we utilize the following result, cf., Lehrenfeld & Olshanskii (2019, Lemma 5.7):

$$\|\boldsymbol{u}_h\|_{\mathcal{O}_{\delta_h}(\Omega_h^n)}^2 \le (1 + c_1(\varepsilon)\Delta t)\|\boldsymbol{u}_h\|_{\Omega_h^n}^2 + c_2(\varepsilon)\nu\Delta t\|\nabla\boldsymbol{u}_h\|_{\Omega_h^n}^2 + c_3(\varepsilon,h)\Delta t Li_h^n(\boldsymbol{u}_h,\boldsymbol{u}_h) \tag{5.16}$$

with $c_1(\varepsilon) = c'c_{\delta_h}w_\infty^n(1+\varepsilon^{-1})$, $c_2(\varepsilon) = c'c_{\delta_h}w_\infty^n\varepsilon/\nu$ and $c_3(\varepsilon) = c'c_{\delta_h}w_\infty^n(\varepsilon+(1+\varepsilon^{-1})h^2)$ and $c' > 0$ independent of h and Δt. Choosing $\varepsilon = \nu c_{L5.5}/(2c'c_{\delta_h}w_\infty^n)$ we then have $c_2 = c_{L5.5}/2$ while we can bound the resulting $c_1(\varepsilon) \le \overline{c}/\nu$, with $\overline{c}$ independent of Δt and h and $c_3 \le \nu c_{L5.5}/2 + h^2\overline{c}/\nu$. This gives the estimate

$$\begin{aligned}\|\boldsymbol{u}_h^{n-1}\|_{\Omega_h^n}^2 &\le \|\boldsymbol{u}_h^{n-1}\|_{\mathcal{O}_{\delta_h}(\Omega_h^{n-1})}^2\\ &\le \left(1 + \frac{\overline{c}\Delta t}{\nu}\right)\|\boldsymbol{u}_h^{n-1}\|_{\Omega_h^{n-1}}^2 + \frac{\nu\Delta t c_{L5.5}}{2}|||\boldsymbol{u}_h^{n-1}|||_{*,n-1}^2 + \frac{\overline{c}h^2}{\nu}\Delta t Li_h^{n-1}(\boldsymbol{u}_h^{n-1},\boldsymbol{u}_h^{n-1}).\end{aligned}$$

Inserting this into (5.15) and summing over $n = 1,\dots,k$ for $k \le N$ then gives for sufficiently small h, such that $\overline{c}h^2 \le 1$

$$\begin{aligned}&\|\boldsymbol{u}_h^k\|_{\Omega_n^k}^2 + \Delta t\sum_{n=1}^{k}\left[\frac{\nu c_{L5.5}}{2}|||\boldsymbol{u}_h^n|||_{*,n}^2 + \frac{L}{\nu}i_h^n(\boldsymbol{u}_h^n,\boldsymbol{u}_h^n)\right]\\ &\quad\le \|\boldsymbol{u}_h^0\|_{\Omega_n^0}^2 + \frac{\nu\Delta t c_{L5.5}}{2}|||\boldsymbol{u}_h^0|||_{*,0}^2 + \frac{L}{\nu}i_h^0(\boldsymbol{u}_h^0,\boldsymbol{u}_h^0) + \Delta t\sum_{n=1}^{k}\frac{c_{P,h}^2}{\nu c_{L5.5}}\|\boldsymbol{f}_h^n\|_{\Omega_h^n}^2 + \Delta t\sum_{n=0}^{k}\frac{\overline{c}}{\nu}\|\boldsymbol{u}_h^n\|_{\Omega_h^n}^2.\end{aligned}$$

Applying a discrete Gronwall inequality with $c_{T5.9\text{a}} = c_{L5.5}$ and $c_{T5.9\text{b}} = \overline{c}$ then gives the desired result. □

Lemma 5.10 For the pressure solution $p_h^n \in Q_h^n$ of (4.1) it holds that

$$\|p_h^n\|_{\Omega_h^n} \le c_{L5.10}\left[\|\frac{1}{\Delta t}(\boldsymbol{u}_h^n - \boldsymbol{u}_h^{n-1})\|_{-1,n} + |||\boldsymbol{u}_h^n|||_{*,n} + \|\boldsymbol{f}_h^n\|_{\Omega_h^n} + j_h^n(p_h^n,p_h^n)^{1/2}\right]. \tag{5.17}$$

Proof. We have that

$$
\begin{aligned}
b_h^n(p_h^n, \boldsymbol{v}_h) &= -\frac{1}{\Delta t}(\boldsymbol{u}_h^n - \boldsymbol{u}_h^{n-1}, \boldsymbol{v}_h)_{\Omega_h^n} - (a_h^n + \nu L i_h^n)(\boldsymbol{u}_h^n, \boldsymbol{v}_h) - {}^1\!/\!_\nu i_h^n(\boldsymbol{u}_h^n, \boldsymbol{v}_h) + \boldsymbol{f}_h^n(\boldsymbol{v}_h) \\
&\leq \left[\| \frac{1}{\Delta t}(\boldsymbol{u}_h^n - \boldsymbol{u}_h^{n-1}) \|_{-1,n} + c(\nu + {}^1\!/\!_\nu) |||\boldsymbol{u}_h^n|||_{*,n} + c_{P,h} \|\boldsymbol{f}_h^n\|_{\Omega_h^n} \right] |||\boldsymbol{v}_h|||_{*,n}.
\end{aligned}
$$

Here we used the continuity of $a_h^n + \nu L i_h^n$, the estimate $i_h^n(\boldsymbol{w}, \boldsymbol{v}) \leq i_h^n(\boldsymbol{w}, \boldsymbol{w})^{1/2} i_h^n(\boldsymbol{v}, \boldsymbol{v})^{1/2}$ with (5.7a) and the Poincaré inequality. The result then follows from the inf-sup result in Lemma 5.6. □

REMARK 5.11 Lemma 5.10 does not immediately result in a satisfactory $\mathcal{L}^2$-stability estimate for the pressure. (5.17) only gives us an estimate for $\Delta t^2 \sum_{n=1}^{k} \|p_h^n\|_{\Omega_h^n}^2$. In order to get a proper estimate of the form $\Delta t \sum_{n=1}^{k} \|p_h^n\|_{\Omega_h^n}^2$ we require an estimate of the term $\frac{1}{\Delta t}\|\boldsymbol{u}_h^n - \boldsymbol{u}_h^{n-1}\|_{-1,n}$, which is independent (of negative powers) of Δt.

5.4 *Geometrical approximation*

We shall assume that we have a higher order approximation of the geometry, i.e.,

$$
\mathrm{dist}(\Omega^n, \Omega_h^n) \leq h^{q+1}
$$

with the geometry approximation order q and that integrals on Ω_h^n can be computed sufficiently accurately. We further assume the existence of a mapping that maps the approximated extended domain to the exact extended domain. In other words, we have $\Phi : \mathcal{O}_{\delta_h}(\Omega_h^n) \to \mathcal{O}_{\delta_h}(\Omega^n)$, which we assume to be well-defined, continuous, it holds that $\Omega^n = \Phi(\Omega_h^n)$, $\Gamma^n = \Phi(\Gamma_h^n)$ and $\mathcal{O}_{\delta_h}(\Omega^n) = \Phi(\mathcal{O}_{\delta_h}(\Omega_h^n))$ and

$$
\|\Phi - \mathrm{Id}\|_{\mathcal{L}^\infty(\mathcal{O}_{\delta_h}(\Omega_h^n))} \lesssim h^{q+1}, \quad \|D\Phi - I\|_{\mathcal{L}^\infty(\mathcal{O}_{\delta_h}(\Omega_h^n))} \lesssim h^q, \quad \|\det(D\Phi) - 1\|_{\mathcal{L}^\infty(\mathcal{O}_{\delta_h}(\Omega_h^n))} \lesssim h^q. \tag{5.18}
$$

Furthermore, for sufficiently small h, the mapping Φ is invertible. Such a mapping has been constructed, e.g., in Gross *et al.* (2015, Section 7.1). This mapping Φ is used here (as in Lehrenfeld & Olshanskii, 2019, and therefore using the same notation) to map from the discrete domain to the exact one. Let $\boldsymbol{v}_h \in \boldsymbol{V}_h^n$ and define $\boldsymbol{v}_h^\ell = \boldsymbol{v}_h \circ \Phi^{-1}$. From the third estimate in (5.18) we have $\det(D\Phi) \simeq 1$, hence we then get using integration by substitution

$$
\|\boldsymbol{v}_h^\ell\|_{\mathcal{O}_{\delta_h}(\Omega^n)}^2 = \sum_{i=1}^{d} \int_{\mathcal{O}_{\delta_h}(\Omega^n)} (\boldsymbol{v}_h^\ell)_i^2 \mathrm{d}\hat{\boldsymbol{x}} = \sum_{i=1}^{d} \int_{\mathcal{O}_{\delta_h}(\Omega_h^n)} \det(D\Phi)(\boldsymbol{v}_h)_i^2 \mathrm{d}\boldsymbol{x} \simeq \|\boldsymbol{v}_h\|_{\mathcal{O}_{\delta_h}(\Omega_h^n)}^2.
$$

Using similar arguments we also have that

$$
\|\boldsymbol{v}_h\|_{\Omega_h^n}^2 \simeq \|\boldsymbol{v}_h^\ell\|_{\Omega^n}^2 \qquad \text{and} \qquad \|\boldsymbol{v}_h\|_{\Gamma_h^n}^2 \simeq \|\boldsymbol{v}_h^\ell\|_{\Gamma^n}^2,
$$

as well as

$$\|\nabla \boldsymbol{v}_h\|^2_{\mathcal{O}_{\delta_h}(\Omega_h^n)} \simeq \|\nabla \boldsymbol{v}_h^\ell\|^2_{\mathcal{O}_{\delta_h}(\Omega^n)} \qquad \text{and} \qquad \|\nabla \boldsymbol{v}_h\|^2_{\Omega_h^n} \simeq \|\nabla \boldsymbol{v}_h^\ell\|^2_{\Omega^n}.$$

For the extension we also have the following result, cf. (Gross *et al.*, 2015, Lemma 7.3):

LEMMA 5.12 The following estimates

$$\|\mathcal{E}\boldsymbol{u} - \boldsymbol{u} \circ \Phi\|_{\Omega_h^n} \lesssim h^{q+1} \|\boldsymbol{u}\|_{\boldsymbol{\mathcal{H}}^1(\Omega^n)}, \tag{5.19a}$$

$$\|\nabla(\mathcal{E}\boldsymbol{u}) - (\nabla\boldsymbol{u}) \circ \Phi\|_{\Omega_h^n} \lesssim h^{q+1} \|\boldsymbol{u}\|_{\boldsymbol{\mathcal{H}}^2(\Omega^n)}, \tag{5.19b}$$

$$\|\mathcal{E}\boldsymbol{u} - \boldsymbol{u} \circ \Phi\|_{\Gamma_h^n} \lesssim h^{q+1} \|\boldsymbol{u}\|_{\boldsymbol{\mathcal{H}}^2(\Omega^n)}, \tag{5.19c}$$

hold for all $\boldsymbol{u} \in \boldsymbol{\mathcal{H}}^2(\Omega^n)$, $n = 1, \ldots, N$. Furthermore, it also holds that

$$\|\mathcal{E}\boldsymbol{u} - (\mathcal{E}\boldsymbol{u}) \circ \Phi\|_{\mathcal{O}_{\delta_h}(\Omega_h^n)} \lesssim h^{q+1} \|\boldsymbol{u}\|_{\boldsymbol{\mathcal{H}}^1(\Omega^n)}. \tag{5.20}$$

Proof. For (5.19a)–(5.19c) we refer to Gross *et al.* (2015, Lemma 7.3). The proof of (5.20) follows the identical lines of (5.19a), but integration over $\mathcal{S}^{\pm}(\Omega_h^n)$ rather that $\mathcal{S}^{\pm}(\Omega_h^n) \setminus \mathcal{S}^{+}(\Omega_h^n)$. □

In the next lemma we state similar estimates to (5.19c) on Γ_h^n, where we however trade a lower regularity of the function on the right-hand side with an only slightly lower convergence rate and an additional (additive) higher order term.

LEMMA 5.13 For all $\boldsymbol{v} \in \boldsymbol{\mathcal{H}}^{m+1}(\Omega^n)$ and $r \in \mathcal{H}^m(\Omega^n)$, $m \geq 1$ we have the estimates

$$h^{1/2}\|\mathcal{E}\partial_{\boldsymbol{n}}\boldsymbol{v} - \partial_{\boldsymbol{n}}\boldsymbol{v} \circ \Phi\|_{\Gamma_h^n} \lesssim h^q \|\boldsymbol{v}\|_{\boldsymbol{\mathcal{H}}^1(\Omega^n)} + h^m \|\boldsymbol{v}\|_{\boldsymbol{\mathcal{H}}^{m+1}(\Omega^n)} \tag{5.21a}$$

$$h^{1/2}\|\mathcal{E}r - r \circ \Phi\|_{\Gamma_h^n} \lesssim h^{q+1} \|r\|_{\mathcal{H}^1(\Omega^n)} + h^m \|r\|_{\mathcal{H}^m(\Omega^n)}. \tag{5.21b}$$

Proof. To make the proof more readable we do not write the extension operator explicitly and identify $\boldsymbol{v}$ with its smooth extension $\mathcal{E}\boldsymbol{v}$. Now let $\boldsymbol{v} \in \boldsymbol{\mathcal{H}}^{m+1}(\Omega^n)$. To prove (5.21a) we insert additive zeros and use the triangle inequality to get

$$\begin{aligned} h^{1/2}\|\partial_{\boldsymbol{n}}\boldsymbol{v} \circ \Phi - \partial_{\boldsymbol{n}}\boldsymbol{v}\|_{\Gamma_h^n} \leq h^{1/2} \Big[&\|\partial_{\boldsymbol{n}}\boldsymbol{v} \circ \Phi - \mathcal{I}^*\partial_{\boldsymbol{n}}\boldsymbol{v} \circ \Phi\|_{\Gamma_h^n} \\ &+ \|\mathcal{I}^*\partial_{\boldsymbol{n}}\boldsymbol{v} \circ \Phi - \mathcal{I}^*\partial_{\boldsymbol{n}}\boldsymbol{v}\|_{\Gamma_h^n} + \|\mathcal{I}^*\partial_{\boldsymbol{n}}\boldsymbol{v} - \partial_{\boldsymbol{n}}\boldsymbol{v}\|_{\Gamma_h^n} \Big]. \end{aligned} \tag{5.22}$$

To bound the first term on the right-hand side of (22) we divide the norm up into the separate contributions of cut elements, use (5.3), the interpolation estimate in Lemma 5.1 as well as Assumption A1 in combination with (5.1) in order to get

$$\|\partial_{\boldsymbol{n}}\boldsymbol{v}\circ\Phi-\mathcal{I}^*\partial_{\boldsymbol{n}}\boldsymbol{v}\circ\Phi\|^2_{\Gamma_h^n}\simeq\|\partial_{\boldsymbol{n}}\boldsymbol{v}-\mathcal{I}^*\partial_{\boldsymbol{n}}\boldsymbol{v}\|^2_{\Gamma^n}=\sum_{K\in\mathscr{T}_{h,\Gamma^n}}\|\partial_{\boldsymbol{n}}\boldsymbol{v}-\mathcal{I}^*\partial_{\boldsymbol{n}}\boldsymbol{v}\|^2_{K\cap\Gamma^n}$$
$$\lesssim\sum_{K\in\mathscr{T}_{h,\Gamma^n}}h^{-1}\|\nabla\boldsymbol{v}-\mathcal{I}^*\nabla\boldsymbol{v}\|^2_K+h^1\|\nabla(\nabla\boldsymbol{v}-\mathcal{I}^*\nabla\boldsymbol{v})\|^2_K$$
$$\lesssim\sum_{K\in\mathscr{T}_{h,\Gamma^n}}h^{2m-1}\|\boldsymbol{v}\|^2_{\boldsymbol{\mathcal{H}}^{m+1}(K)}+h^{2m-1}\|\boldsymbol{v}\|^2_{\boldsymbol{\mathcal{H}}^{m+1}(K)}\lesssim h^{2m-1}\|\boldsymbol{v}\|^2_{\boldsymbol{\mathcal{H}}^{m+1}(\mathcal{O}^n_{\delta_h,\mathscr{T}})}\lesssim h^{2m-1}\|\boldsymbol{v}\|^2_{\boldsymbol{\mathcal{H}}^{m+1}(\Omega^n)}. \tag{5.23}$$

The third term in (22) can be estimated completely analogously. For the second term we make use of the fact that the argument of the norm is discrete, therefore permitting the use of the inverse estimate (5.2a). Then with (5.2c) and (5.1) it follows that

$$\|\mathcal{I}^*\partial_{\boldsymbol{n}}\boldsymbol{v}\circ\Phi-\mathcal{I}^*\partial_{\boldsymbol{n}}\boldsymbol{v}\|^2_{\Gamma_h^n}=\sum_{K\in\mathscr{T}_{h,\Gamma_h^n}}\|\mathcal{I}^*\partial_{\boldsymbol{n}}\boldsymbol{v}\circ\Phi-\mathcal{I}^*\partial_{\boldsymbol{n}}\boldsymbol{v}\|^2_{K\cap\Gamma_h^n}\lesssim\sum_{K\in\mathscr{T}_{h,\Gamma_h^n}}h^{-1}\|\nabla(\mathcal{I}^*\boldsymbol{v}\circ\Phi-\mathcal{I}^*\boldsymbol{v})\|^2_K$$
$$\lesssim\sum_{K\in\mathscr{T}_{h,\Gamma_h^n}}h^{-3}\|\mathcal{I}^*(\boldsymbol{v}\circ\Phi-\boldsymbol{v})\|^2_K\lesssim h^{-3}\|\boldsymbol{v}\circ\Phi-\boldsymbol{v}\|^2_{\mathcal{O}_{\delta_h}(\Omega_h^n)}\lesssim h^{2q-1}\|\boldsymbol{v}\|^2_{\boldsymbol{\mathcal{H}}^1(\Omega^n)}, \tag{5.24}$$

where we made use of (5.20) in the last step. Combining (5.23) and (5.24) then gives us the desired estimate

$$h^{1/2}\|\partial_{\boldsymbol{n}}\boldsymbol{v}\circ\Phi-\partial_{\boldsymbol{n}}\boldsymbol{v}\|_{\Gamma_h^n}\lesssim h^m\|\boldsymbol{v}\|_{\boldsymbol{\mathcal{H}}^{m+1}(\Omega^n)}+h^q\|\boldsymbol{v}\|_{\boldsymbol{\mathcal{H}}^1(\Omega^n)}.$$

For the proof of (5.21b) we again identify r with $\mathcal{E}r$. Now let $r\in\mathcal{H}^m(\Omega^n)$. We split the term as before, i.e., replace $\partial_{\boldsymbol{n}}\boldsymbol{v}$ with r in (22), to get

$$h^{1/2}\|r\circ\Phi-r\|_{\Gamma_h^n}\le h^{1/2}\Big[\|r\circ\Phi-\mathcal{I}^*r\circ\Phi\|_{\Gamma_h^n}+\|\mathcal{I}^*r\circ\Phi-\mathcal{I}^*r\|_{\Gamma_h^n}+\|\mathcal{I}^*r-r\|_{\Gamma_h^n}\Big]. \tag{5.25}$$

For the first and third term we can proceed as in (5.23), with the only difference that in the application of Lemma 5.1 results in a $\mathcal{H}^m(\Omega^n)$-norm, i.e.,

$$\|r\circ\Phi-\mathcal{I}^*r\circ\Phi\|^2_{\Gamma_h^n}\lesssim h^{2m-1}\|r\|^2_{\mathcal{H}^m(\Omega^n)}\qquad\text{and}\qquad\|\mathcal{I}^*r-r\|^2_{\Gamma_h^n}\lesssim h^{2m-1}\|r\|^2_{\mathcal{H}^m(\Omega^n)}.$$

For the middle term in (5.25) we use the trace estimate (5.3), the inverse estimate (5.2a) and the estimate (5.20) with (5.1) to obtain

$$\|\mathcal{I}^*r\circ\Phi-\mathcal{I}^*r\|^2_{\Gamma_h^n}\lesssim\sum_{K\in\mathscr{T}_{h,\Gamma_h^n}}h^{-1}\|\mathcal{I}^*r\circ\Phi-\mathcal{I}^*r\|^2_K+h^1\|\nabla(\mathcal{I}^*r\circ\Phi-\mathcal{I}^*r)\|^2_K$$
$$\lesssim\sum_{K\in\mathscr{T}_{h,\Gamma_h^n}}h^{-1}\|\mathcal{I}^*(r\circ\Phi-r)\|^2_K\lesssim h^{-1}\|r\circ\Phi-r\|^2_{\mathcal{O}_{\delta_h}(\Omega_h^n)}\lesssim h^{2q+1}\|r\|^2_{\mathcal{H}^1(\Omega^n)}.$$

Combining these two estimates shows the desired result. □

5.5 *Consistency*

Using integration by parts we see that any smooth solution $(\boldsymbol{u}, p)$ to the strong problem (2.1) fulfils

$$\int_{\Omega^n} \partial_t \boldsymbol{u}(t_n)\boldsymbol{v}_h^\ell \mathrm{d}\hat{\boldsymbol{x}} + a_1^n(\boldsymbol{u}(t_n), \boldsymbol{v}_h^\ell) + b_1^n(p(t_n), \boldsymbol{v}_h^\ell) + b_1^n(q_h^\ell, \boldsymbol{u}(t_n)) = \boldsymbol{f}^n(\boldsymbol{v}_h^\ell) \tag{5.26}$$

for the test-functions $(\boldsymbol{v}_h^\ell, q_h^\ell) = (\boldsymbol{v}_h \circ \Phi^{-1}, q_h \circ \Phi^{-1})$ with $(\boldsymbol{v}_h, q_h) \in \boldsymbol{V}_h^n \times Q_h^n$, the mapping Φ from Section 5.4 and the bilinear forms

$$a_1^n(\boldsymbol{u}, \boldsymbol{v}) := a^n(\boldsymbol{u}, \boldsymbol{v}) + \nu \int_{\Gamma^n} (-\partial_{\boldsymbol{n}} \boldsymbol{u}) \cdot \boldsymbol{v} \, \mathrm{d}s$$

and

$$b_1^n(p, \boldsymbol{v}) := b^n(p, \boldsymbol{v}) + \int_{\Gamma^n} p\boldsymbol{v} \cdot \boldsymbol{n} \mathrm{d}s,$$

where we recall the bilinear forms $a^n(\cdot,\cdot)$ and $b^n(\cdot,\cdot)$ with respect to Ω^n from (3.2). For simplicity of notation we shall identify the smooth extension $\mathcal{E}\boldsymbol{u}$ with $\boldsymbol{u}$, and denote $\mathbb{E}^n := \boldsymbol{u}^n - \boldsymbol{u}_h^n$ and $\mathbb{D}^n := p^n - p_h^n$. Since $\Omega_h^n \subset \mathcal{O}_\delta(\Omega(t))$, $t \in [t_{n-1}, t_n]$, $\boldsymbol{u}(t_{n-1}) = \boldsymbol{u}^{n-1}$ is well defined on Ω_h^n. Subtracting (4.1) from (5.26), and adding and subtracting appropriate terms, we obtain the error equation

$$\begin{aligned}
&\int_{\Omega_h^n} \frac{\mathbb{E}^n - \mathbb{E}^{n-1}}{\Delta t} \cdot \boldsymbol{v}_h \mathrm{d}\boldsymbol{x} + a_h^n(\mathbb{E}^n, \boldsymbol{v}_h) + b_h^n(\mathbb{D}^n, \boldsymbol{v}_h) + b_h^n(q_h, \mathbb{E}^n) + s_h^n((\mathbb{E}^n, \mathbb{D}^n), (\boldsymbol{v}_h, q_h)) \\
&\quad = \boldsymbol{f}^n(\boldsymbol{v}_h^\ell) - \boldsymbol{f}_h^n(\boldsymbol{v}_h) + \int_{\Omega_h^n} \frac{\boldsymbol{u}^n - \boldsymbol{u}^{n-1}}{\Delta t} \cdot \boldsymbol{v}_h \mathrm{d}\boldsymbol{x} - \int_{\Omega^n} \partial_t \boldsymbol{u}^n \cdot \boldsymbol{v}_h^\ell \mathrm{d}\hat{\boldsymbol{x}} + a_h^n(\boldsymbol{u}^n, \boldsymbol{v}_h) - a_1^n(\boldsymbol{u}^n, \boldsymbol{v}_h^\ell) \\
&\qquad\qquad b_h^n(p^n, \boldsymbol{v}_h) - b_1^n(p^n, \boldsymbol{v}_h^\ell) + b_h^n(q_h, \boldsymbol{u}^n) - b_1^n(q_h^\ell, \boldsymbol{u}^n) + s_h^n((\boldsymbol{u}^n, p^n), (\boldsymbol{v}_h, q_h)) \\
&\quad = \mathfrak{T}_1 + \mathfrak{T}_2 + \mathfrak{T}_3 + \mathfrak{T}_4 + \mathfrak{T}_5 + \mathfrak{T}_6 \\
&\quad = \mathfrak{E}_c^n(\boldsymbol{v}_h, q_h).
\end{aligned} \tag{5.27}$$

These six terms correspond to the forcing, time derivative, diffusion, pressure, divergence constraint and ghost-penalty contributions, respectively.

LEMMA 5.14 (Consistency estimate). The consistency error has the bound

$$|\mathfrak{E}_c^n((\boldsymbol{v}_h, q_h))| \lesssim \left(\Delta t + h^q + \frac{h^m L^{1/2}}{\nu}\right) R_{c,1}(\boldsymbol{u}, p, \boldsymbol{f}) |||\boldsymbol{v}_h|||_{*,n} + (h^q + h^m) R_{c,2}(\boldsymbol{u}, p) |||q_h|||_{*,n}$$

with

$$R_{c,1}(\boldsymbol{u}, p, \boldsymbol{f}) = \|\boldsymbol{u}\|_{\boldsymbol{\mathcal{W}}^{2,\infty}(\mathcal{Q})} + \|\boldsymbol{f}^n\|_{\boldsymbol{\mathcal{H}}^1(\Omega^n)} + \sup_{t \in [0,T]} \left(\|\boldsymbol{u}(t)\|_{\boldsymbol{\mathcal{H}}^{m+1}(\Omega(t))} + \|p(t)\|_{\mathcal{H}^m(\Omega(t))} \right)$$

and

$$R_{c,2}(\boldsymbol{u},p) = \sup_{t\in[0,T]} \left(\|\boldsymbol{u}(t)\|_{\boldsymbol{\mathcal{H}}^{m+1}(\Omega(t))} + \|p(t)\|_{\mathcal{H}^m(\Omega(t))}\right).$$

Proof. We estimate each of the six components of the consistency error separately, making use of results from the literature where possible. The first preprint version (von Wahl *et al.*, 2020) of this paper includes the complete set of steps.

Consistency term 1: $\mathfrak{T}_1 = \boldsymbol{f}^n(\boldsymbol{v}_h^\ell) - \boldsymbol{f}_h^n(\boldsymbol{v}_h)$: Using (5.18), Lemma 5.12 and Assumption A1 we have

$$|\mathfrak{T}_1| = |\boldsymbol{f}^n(\boldsymbol{v}_h^\ell) - \boldsymbol{f}_h^n(\boldsymbol{v}_h)| \lesssim h^q \|\boldsymbol{f}^n\|_{\boldsymbol{\mathcal{H}}^1(\Omega^n)} \|\boldsymbol{v}_h\|_{\Omega_h^n}. \tag{5.28}$$

See Gross *et al.* (2014, Lemma 7.5), the preprint of Gross *et al.* (2015), for a proof thereof.

Consistency term 2: $\mathfrak{T}_2 = \int_{\Omega_h^n} \frac{\boldsymbol{u}^n - \boldsymbol{u}^{n-1}}{\Delta t} \cdot \boldsymbol{v}_h \,\mathrm{d}\boldsymbol{x} - \int_{\Omega^n} \partial_t \boldsymbol{u}^n \cdot \boldsymbol{v}_h^\ell \,\mathrm{d}\hat{\boldsymbol{x}}$: For the time derivative we have the consistency estimate

$$|\mathfrak{T}_2| \lesssim (\Delta t + h^q) \|\boldsymbol{u}\|_{\boldsymbol{\mathcal{W}}^{2,\infty}(Q)} \|\boldsymbol{v}_h\|_{\Omega_h^n}. \tag{5.29}$$

The proof for this can be found in Lehrenfeld & Olshanskii (2019, Lemma 5.11).

Consistency term 3: $\mathfrak{T}_3 = a_h^n(\boldsymbol{u}^n, \boldsymbol{v}_h) - a_1^n(\boldsymbol{u}^n, \boldsymbol{v}_h^\ell)$: For the volume integral part in the diffusion consistency error term $\mathfrak{T}_3$ we have from Gross *et al.* (2015, Lemma 7.4) that

$$|\mathfrak{I}_3^1| = \left| \int_{\Omega_h^n} \nu \nabla \boldsymbol{u}^n : \nabla \boldsymbol{v}_h \,\mathrm{d}\boldsymbol{x} - \int_{\Omega^n} \nu \nabla \boldsymbol{u}^n : \nabla \boldsymbol{v}_h^\ell \,\mathrm{d}\hat{\boldsymbol{x}} \right| \lesssim h^q \|\boldsymbol{u}\|_{\boldsymbol{\mathcal{W}}^{2,\infty}(Q)} \|\nabla \boldsymbol{v}_h\|_{\Omega_h^n}.$$

Before we estimate the boundary contribution we observe that it follows from the chain rule that

$$\nabla \boldsymbol{v}_h^\ell(\hat{\boldsymbol{x}}) = \nabla(\boldsymbol{v}_h \circ \Phi^{-1})(\hat{\boldsymbol{x}}) = \nabla \boldsymbol{v}_h(\boldsymbol{x}) D\Phi(\boldsymbol{x})^{-1} \qquad \text{for } \boldsymbol{x} \in \Omega^n,\ \boldsymbol{x} := \Phi^{-1}(\hat{\boldsymbol{x}}). \tag{5.30}$$

Furthermore, due to (5.18), we have

$$\|I - JD\Phi^{-1}\|_{\boldsymbol{\mathcal{L}}^\infty(\mathcal{O}_{\delta_h}(\Omega_h^n))} \leq \|(I - IJ)D\Phi^{-1}\|_{\boldsymbol{\mathcal{L}}^\infty(\mathcal{O}_{\delta_h}(\Omega_h^n))} + \|I - D\Phi^{-1}\|_{\boldsymbol{\mathcal{L}}^\infty(\mathcal{O}_{\delta_h}(\Omega_h^n))} \lesssim h^q. \tag{5.31}$$

Now we split the boundary contributions from $\mathfrak{T}_3 = a_h^n(\boldsymbol{u}^n, \boldsymbol{v}_h) - a_1^n(\boldsymbol{u}^n, \boldsymbol{v}_h^\ell)$ into three parts

$$\underbrace{-\int_{\Gamma_h^n} \nu \partial_{\boldsymbol{n}} \boldsymbol{u}^n \cdot \boldsymbol{v}_h \,\mathrm{d}s + \int_{\Gamma^n} \nu \partial_{\boldsymbol{n}} \boldsymbol{u}^n \cdot \boldsymbol{v}_h^\ell \,\mathrm{d}\hat{s}}_{\mathfrak{I}_3^2} \underbrace{- \int_{\Gamma_h^n} \nu \partial_{\boldsymbol{n}} \boldsymbol{v}_h \cdot \boldsymbol{u}^n \,\mathrm{d}s}_{\mathfrak{I}_3^3} \underbrace{+ \frac{\sigma}{h} \int_{\Gamma_h^n} \nu \boldsymbol{u}^n \cdot \boldsymbol{v}_h \,\mathrm{d}s}_{\mathfrak{I}_3^4}.$$

For $\mathfrak{I}_3^2$ we use integration by substitution, the third bound in (5.18) and Lemma 5.12, which gives

$$\begin{aligned}
\mathfrak{I}_3^2 &= -\int_{\Gamma_h^n} \nu\partial_{\boldsymbol{n}}\boldsymbol{u}^n \cdot \boldsymbol{v}_h \mathrm{d}\,s + \int_{\Gamma^n} \nu\partial_{\boldsymbol{n}}\boldsymbol{u}^n \cdot \boldsymbol{v}_h^\ell \mathrm{d}\,\hat{s} = -\int_{\Gamma_h^n} \nu\partial_{\boldsymbol{n}}\boldsymbol{u}^n \cdot \boldsymbol{v}_h \mathrm{d}\,s + \int_{\Gamma_h^n} \nu\partial_{\boldsymbol{n}}\boldsymbol{u}^n \circ \Phi \cdot J\boldsymbol{v}_h \mathrm{d}\,s \\
&= \int_{\Gamma_h^n} \nu\partial_{\boldsymbol{n}}\boldsymbol{u}^n \cdot (J-1)\boldsymbol{v}_h \mathrm{d}\,s + \int_{\Gamma_h^n} \nu(\partial_{\boldsymbol{n}}\boldsymbol{u}^n \circ \Phi - \partial_{\boldsymbol{n}}\boldsymbol{u}^n) \cdot J\boldsymbol{v}_h \mathrm{d}\,s \\
&\lesssim h^q \|h^{1/2}\partial_{\boldsymbol{n}}\boldsymbol{u}^n\|_{\Gamma_h^n} \|h^{-1/2}\boldsymbol{v}_h\|_{\Gamma_h^n} + h^{1/2}\|\partial_{\boldsymbol{n}}\boldsymbol{u}^n \circ \Phi - \partial_{\boldsymbol{n}}\boldsymbol{u}^n\|_{\Gamma_h^n} \|h^{-1/2}\boldsymbol{v}_h\|_{\Gamma_h^n}.
\end{aligned}$$

Using the standard trace inequality we have together with Assumption A1

$$\|\partial_{\boldsymbol{n}}\boldsymbol{u}^n\|_{\Gamma_h^n} \lesssim \|\boldsymbol{u}^n\|_{\boldsymbol{\mathcal{H}}^2(\Omega_h^n)} \lesssim \|\boldsymbol{u}^n\|_{\boldsymbol{\mathcal{H}}^2(\mathcal{O}_\delta(\Omega^n))} \lesssim \|\boldsymbol{u}^n\|_{\boldsymbol{\mathcal{H}}^2(\Omega^n)}.$$

Combining this result with (5.21a) now gives the estimate

$$|\mathfrak{I}_3^2| \lesssim h^q \|\boldsymbol{u}^n\|_{\boldsymbol{\mathcal{H}}^2(\Omega^n)} \|h^{-1/2}\boldsymbol{v}_h\|_{\Gamma_h^n} + \left[h^m \|\boldsymbol{u}^n\|_{\boldsymbol{\mathcal{H}}^{m+1}(\Omega^n)} + h^q \|\boldsymbol{u}^n\|_{\boldsymbol{\mathcal{H}}^1(\Omega^n)}\right] \|h^{-1/2}\boldsymbol{v}_h\|_{\Gamma_h^n}.$$

For the term $\mathfrak{I}_3^3$ we use the fact that $\boldsymbol{u}^n$ vanishes on Γ^n, so that with (5.29), (5.30) and (5.19c)

$$\begin{aligned}
\mathfrak{I}_3^3 &= \int_{\Gamma^n} \nu\partial_{\boldsymbol{n}}\boldsymbol{v}_h^\ell \cdot \boldsymbol{u}^n \mathrm{d}\,\hat{s} - \int_{\Gamma_h^n} \nu\partial_{\boldsymbol{n}}\boldsymbol{v}_h \cdot \underbrace{\boldsymbol{u}^n}_{=0} \mathrm{d}\,s = \int_{\Gamma_h^n} \nu J\partial_{\boldsymbol{n}}\boldsymbol{v}_h D\Phi^{-1} \cdot \boldsymbol{u}^n \circ \Phi \mathrm{d}\,s - \int_{\Gamma_h^n} \nu\partial_{\boldsymbol{n}}\boldsymbol{v}_h \cdot \boldsymbol{u}^n \mathrm{d}\,s \\
&= \int_{\Gamma_h^n} \nu J\partial_{\boldsymbol{n}}\boldsymbol{v}_h D\Phi^{-1} \cdot (\boldsymbol{u}^n \circ \Phi - \boldsymbol{u}^n)\mathrm{d}\,s + \int_{\Gamma_h^n} \nu\partial_{\boldsymbol{n}}\boldsymbol{v}_h(I - JD\Phi^{-1}) \cdot \boldsymbol{u}^n \mathrm{d}\,s \\
&\lesssim h^{q+1/2}\|h^{1/2}\partial_{\boldsymbol{n}}\boldsymbol{v}_h\|_{\Gamma_h^n} \|\boldsymbol{u}^n\|_{\boldsymbol{\mathcal{H}}^2(\Omega^n)} + h^q \|h^{1/2}\partial_{\boldsymbol{n}}\boldsymbol{v}_h\|_{\Gamma_h^n} \|h^{-1/2}\boldsymbol{u}^n\|_{\Gamma_h^n}.
\end{aligned}$$

Using the trace estimate (5.2c) we have for the first boundary norm

$$\|h^{1/2}\partial_{\boldsymbol{n}}\boldsymbol{v}_h\|_{\Gamma_h^n} = \sum_{T\in\mathcal{T}_{h,\Gamma_h^n}} \|h^{1/2}\partial_{\boldsymbol{n}}\boldsymbol{v}_h\|_{T\cap\Gamma_h^n} \lesssim \sum_{T\in\mathcal{T}_{h,\Gamma_h^n}} \|\nabla\boldsymbol{v}_h\|_T \lesssim \|\nabla\boldsymbol{v}_h\|_{\mathcal{O}^n_{\delta_h,\mathcal{T}}}.$$

Furthermore, we can estimate $\|h^{-1/2}\boldsymbol{u}^n\|_{\Gamma_h^n}$ using the fact that $\boldsymbol{u}^n \circ \Phi(\boldsymbol{x}) = 0$ for $\boldsymbol{x} \in \Gamma_h^n$ and (5.19c) to get

$$\|h^{-1/2}\boldsymbol{u}^n\|_{\Gamma_h^n} \le h^{-1/2}\Big[\|\boldsymbol{u}^n - \boldsymbol{u}^n \circ \Phi\|_{\Gamma_h^n} + \underbrace{\|\boldsymbol{u}^n \circ \Phi\|_{\Gamma_h^n}}_{=0}\Big] \lesssim h^{q+1/2}\|\boldsymbol{u}^n\|_{\boldsymbol{\mathcal{H}}^2(\Omega^n)}. \tag{5.32}$$

These two estimates then give the bound

$$|\mathfrak{I}_3^3| \lesssim h^{q+1/2}\|\boldsymbol{u}^n\|_{\boldsymbol{\mathcal{H}}^2(\Omega^n)} \|\nabla\boldsymbol{v}_h\|_{\mathcal{O}^n_{\delta_h,\mathcal{T}}}.$$

For the penalty term $\mathfrak{I}_3^4$ we proceed as for $\mathfrak{I}_3^3$ using (5.31):

$$
\begin{aligned}
\mathfrak{I}_3^4 &= \nu\frac{\sigma}{h}\int_{\Gamma_h^n}\underbrace{\boldsymbol{u}^n}_{=0}\cdot\boldsymbol{v}_h\,\mathrm{d}s - \frac{\sigma}{h}\int_{\Gamma^n}\boldsymbol{u}^n\cdot\boldsymbol{v}_h^\ell\,\mathrm{d}\hat{s} = \nu\frac{\sigma}{h}\int_{\Gamma_h^n}\boldsymbol{u}^n\cdot\boldsymbol{v}_h - \boldsymbol{u}^n\circ\Phi\cdot J\boldsymbol{v}_h\,\mathrm{d}s \\
&= \nu\frac{\sigma}{h}\int_{\Gamma_h^n}(\boldsymbol{u}^n - \boldsymbol{u}^n\circ\Phi)\cdot J\boldsymbol{v}_h + \boldsymbol{u}^n\cdot(1-J)\boldsymbol{v}_h\,\mathrm{d}s \lesssim h^q\left[\|\boldsymbol{u}^n\|_{\boldsymbol{\mathcal{H}}^2(\Omega^n)} + \|h^{-1/2}\boldsymbol{u}^n\|_{\Gamma_h^n}\right]\|h^{-1/2}\boldsymbol{v}_h\|_{\Gamma_h^n} \\
&\lesssim h^q\|\boldsymbol{u}^n\|_{\boldsymbol{\mathcal{H}}^2(\Omega^n)}\|h^{-1/2}\boldsymbol{v}_h\|_{\Gamma_h^n}.
\end{aligned}
$$

Combining these estimates then gives the bound on $\mathfrak{T}_3$ as

$$
|\mathfrak{T}_3| \le |\mathfrak{I}_3^1| + |\mathfrak{I}_3^2| + |\mathfrak{I}_3^3| + |\mathfrak{I}_3^4| \lesssim h^q\|\boldsymbol{u}\|_{\boldsymbol{\mathcal{W}}^{2,\infty}(Q)}|||\boldsymbol{v}_h|||_{*,n} + h^m\|\boldsymbol{u}^n\|_{\boldsymbol{\mathcal{H}}^{m+1}(\Omega^n)}\|h^{-1/2}\boldsymbol{v}_h\|_{\Gamma_h^n}. \tag{5.33}
$$

<u>Consistency term 4:</u> $\mathfrak{T}_4 = b_h^n(p^n, \boldsymbol{v}_h) - b_1^n(p^n, \boldsymbol{v}_h^\ell)$: As in (5.29), for the divergence we have

$$
\nabla\cdot\boldsymbol{v}_h^\ell(\hat{\boldsymbol{x}}) = \mathrm{tr}(\nabla(\boldsymbol{v}_h\circ\Phi^{-1})(\hat{\boldsymbol{x}})) = \mathrm{tr}(\nabla\boldsymbol{v}_h(\boldsymbol{x})D\Phi(\boldsymbol{x})^{-1}) \qquad \text{for } \boldsymbol{x}\in\Omega^n,\ \boldsymbol{x} := \Phi^{-1}(\hat{\boldsymbol{x}}).
$$

We split the pressure term $\mathfrak{T}_4 = \mathfrak{I}_4^1 + \mathfrak{I}_4^2$ into volume and boundary integrals, respectively. The volume term can then be rewritten as

$$
\begin{aligned}
\mathfrak{I}_4^1 &:= -\int_{\Omega_h^n}p^n\nabla\cdot\boldsymbol{v}_h\,\mathrm{d}\boldsymbol{x} + \int_{\Omega^n}p^n\nabla\cdot\boldsymbol{v}_h^\ell\,\mathrm{d}\hat{\boldsymbol{x}} = \int_{\Omega_h^n} -p^n\nabla\cdot\boldsymbol{v}_h + p^n\circ\Phi\,\mathrm{tr}(\nabla\boldsymbol{v}_hD\Phi^{-1})J\,\mathrm{d}\boldsymbol{x} \\
&= \int_{\Omega_h^n}\left[p^n(J-1)\nabla\cdot\boldsymbol{v}_h\right] + \left[(p^n\circ\Phi - p^n)\mathrm{tr}(\nabla\boldsymbol{v}_hD\Phi^{-1})J\right] + \left[p^nJ\mathrm{tr}(\nabla\boldsymbol{v}_hD\Phi^{-1} - \nabla\boldsymbol{v}_h)\right]\mathrm{d}\boldsymbol{x} \\
&\lesssim h^q\|p^n\|_{\Omega_h^n}\|\nabla\boldsymbol{v}_h\|_{\Omega_h^n} + h^{q+1}\|p^n\|_{\mathcal{H}^1(\Omega^n)}\|\nabla\boldsymbol{v}_h\|_{\Omega_h^n} + h^q\|p^n\|_{\Omega_h^n}\|\nabla\boldsymbol{v}_h\|_{\Omega_h^n} \lesssim h^q\|p^n\|_{\mathcal{H}^1(\Omega^n)}\|\nabla\boldsymbol{v}_h\|_{\Omega_h^n}.
\end{aligned}
$$

For the boundary terms we have

$$
\begin{aligned}
\mathfrak{I}_4^2 &:= \int_{\Gamma_h^n}p^n\boldsymbol{v}_h\cdot\boldsymbol{n}\,\mathrm{d}s - \int_{\Gamma^n}p^n\boldsymbol{v}_h^\ell\cdot\boldsymbol{n}\,\mathrm{d}\hat{s} = \int_{\Gamma_h^n}p^n\boldsymbol{v}_h\cdot\boldsymbol{n}\,\mathrm{d}s - \int_{\Gamma_h^n}p^n\circ\Phi\,\boldsymbol{v}_h\cdot\boldsymbol{n}J\,\mathrm{d}s \\
&= \int_{\Gamma_h^n}p^n\boldsymbol{v}_h\cdot\boldsymbol{n}(1-J)\,\mathrm{d}s + \int_{\Gamma_h^n}(p^n - p^n\circ\Phi)\,\boldsymbol{v}_h\cdot\boldsymbol{n}J\,\mathrm{d}s \lesssim h^q\|p^n\|_{\Gamma_h^n}\|\boldsymbol{v}\|_{\Gamma_h^n} + \|p^n - p^n\circ\Phi\|_{\Gamma_h^n}\|\boldsymbol{v}\|_{\Gamma_h^n}.
\end{aligned} \tag{5.34}
$$

For the pressure part in the first of these terms two term we observe that using (5.3) and Assumption A1 gives us

$$
\|p^n\|_{\Gamma_h^n}^2 = \sum_{K\in\mathscr{T}_{h,\Gamma_h^n}}\|p^n\|_{K\cap\Gamma_h^n}^2 \lesssim \sum_{K\in\mathscr{T}_{h,\Gamma_h^n}}\left[h^{-1}\|p^n\|_K^2 + h\|\nabla p^n\|_K^2\right] \lesssim h^{-1}\|p^n\|_{\mathcal{H}^1(\mathcal{O}_{\delta_h}(\Omega^n))}^2 \lesssim h^{-1}\|p^n\|_{\mathcal{H}^1(\Omega^n)}.
$$

For the pressure part in the second summand of (5.33) we apply (5.21b). Combining these results then gives

$$|\mathfrak{I}_4^2| \lesssim h^q \|p^n\|_{\mathcal{H}^1(\Omega^n)} \|h^{-1/2}\boldsymbol{v}_h\|_{\Gamma_h^n} + h^m \|p^n\|_{\mathcal{H}^m(\Omega^n)} \|h^{-1/2}\boldsymbol{v}_h\|_{\Gamma_h^n}.$$

Together, these estimates then give us the bound

$$|\mathfrak{T}_4| \lesssim h^q \|p^n\|_{\mathcal{H}^1(\Omega^n)} |||\boldsymbol{v}_h|||_{*,n} + h^m \|p^n\|_{\mathcal{H}^m(\Omega^n)} \|h^{-1/2}\boldsymbol{v}_h\|_{\Gamma_h^n}. \tag{5.35}$$

Consistency term 5: $\mathfrak{T}_5 = b_h^n(q_h, \boldsymbol{u}^n) - b_1^n(q_h^\ell, \boldsymbol{u}^n)$: The volume terms of the divergence constraint can again be rewritten as

$$\begin{aligned}
\mathfrak{I}_5^1 &:= -\int_{\Omega_h^n} q_h \nabla\cdot\boldsymbol{u}^n \mathrm{d}\boldsymbol{x} + \int_{\Omega^n} q_h^\ell \nabla\cdot\boldsymbol{u}^n \mathrm{d}\hat{\boldsymbol{x}} = \int_{\Omega_h^n} -q_h\nabla\cdot\boldsymbol{u}^n + q_h \nabla\cdot\boldsymbol{u}^n \circ \Phi J \mathrm{d}\boldsymbol{x} \\
&= \int_{\Omega_h^n} q_h \nabla\cdot\boldsymbol{u}^n (J-1)\mathrm{d}\boldsymbol{x} + \int_{\Omega_h^n} q_h(\nabla\cdot\boldsymbol{u}^n\circ\Phi - \nabla\cdot\boldsymbol{u}^n) J \mathrm{d}\boldsymbol{x}.
\end{aligned}$$

$\mathfrak{I}_5^1$ can then be bounded again using (5.18) and Lemma 5.12

$$\begin{aligned}
|\mathfrak{I}_5^1| &\lesssim h^q \|q_h\|_{\Omega_h^n} \|\nabla\boldsymbol{u}^n\|_{\Omega_h^n} + \|q_h\|_{\Omega_h^n} \|\nabla\boldsymbol{u}^n\circ\Phi - \nabla\boldsymbol{u}^n\|_{\Omega_h^n} \\
&\lesssim h^q \|q_h\|_{\Omega_h^n} \|\nabla\boldsymbol{u}^n\|_{\Omega_h^n} + h^{q+1}\|q_h\|_{\Omega_h^n} \|\boldsymbol{u}^n\|_{\boldsymbol{\mathcal{H}}^2(\Omega^n)} \lesssim h^q \|q_h\|_{\Omega_h^n} \|\boldsymbol{u}^n\|_{\boldsymbol{\mathcal{H}}^2(\Omega^n)}.
\end{aligned}$$

The boundary contribution in $\mathfrak{T}_5$ are

$$\begin{aligned}
\mathfrak{I}_5^2 &:= \int_{\Gamma_h^n} q_h \boldsymbol{u}^n\cdot\boldsymbol{n}\mathrm{d}s - \int_{\Gamma^n} q_h^\ell \boldsymbol{u}^n\cdot\boldsymbol{n}\mathrm{d}\hat{s} = \int_{\Gamma_h^n} q_h \left(\boldsymbol{u}^n\cdot\boldsymbol{n} - (\boldsymbol{u}^n\cdot\boldsymbol{n})\circ\Phi J\right)\mathrm{d}s \\
&= \int_{\Gamma_h^n} q_h(\boldsymbol{u}^n\cdot\boldsymbol{n} - (\boldsymbol{u}^n\cdot\boldsymbol{n})\circ\Phi) J\mathrm{d}s + \int_{\Gamma_h^n} q_h\boldsymbol{u}^n\cdot\boldsymbol{n}(1-J)\mathrm{d}s \\
&\lesssim \|q_h\|_{\Gamma_h^n} \|\boldsymbol{u}^n\cdot\boldsymbol{n} - (\boldsymbol{u}^n\cdot\boldsymbol{n})\circ\Phi\|_{\Gamma_h^n} + h^q \|q_h\|_{\Gamma_h^n} \|\boldsymbol{u}^n\cdot\boldsymbol{n}\|_{\Gamma_h^n}.
\end{aligned}$$

We have, due to the homogeneous Dirichlet conditions, that

$$\|\boldsymbol{u}^n\cdot\boldsymbol{n}\|_{\Gamma_h^n} \le \|\boldsymbol{u}^n\cdot\boldsymbol{n} - (\boldsymbol{u}^n\cdot\boldsymbol{n})\circ\Phi\|_{\Gamma_h^n} + \overbrace{\|\boldsymbol{u}^n\cdot\boldsymbol{n}\circ\Phi\|_{\Gamma_h^n}}^{=0}.$$

For the term $\|\boldsymbol{u}^n\cdot\boldsymbol{n} - (\boldsymbol{u}^n\cdot\boldsymbol{n})\circ\Phi\|_{\Gamma_h^n}$ we can then apply (5.19c). Combining these results then gives us the bound

$$|\mathfrak{I}_5^2| \lesssim (1+h^q)h^{q+1/2}\|\boldsymbol{u}^n\|_{\boldsymbol{\mathcal{H}}^2(\Omega^n)} \|q_h\|_{\mathcal{O}^n_{\delta_h,\mathcal{T}}},$$

where we made use of the trace estimate (5.3) and the inverse estimate (5.2a) to bound $\|q_h\|_{\Gamma_h^n} \lesssim h^{-1/2}\|q_h\|_{\mathcal{O}^n_{\delta_h,\mathscr{T}}}$. These bounds on the volume and the boundary contributions of $\mathfrak{T}_5$ then give

$$|\mathfrak{T}_5| \lesssim h^q \|\boldsymbol{u}^n\|_{\boldsymbol{\mathcal{H}}^2(\Omega^n)} |||q_h|||_{*,n} + h^m \|\boldsymbol{u}^n\|_{\boldsymbol{\mathcal{H}}^{m+1}(\Omega^n)} |||q_h|||_{*,n}. \tag{5.36}$$

Consistency term 6: $\mathfrak{T}_6 = s_h^n((\boldsymbol{u}^n, p^n), (\boldsymbol{v}_h, q_h))$: To bound $|\mathfrak{T}_6|$ we use the Cauchy–Schwartz inequality, Lemma 4.1 and Assumption A1 to get

$$\begin{aligned}
|\mathfrak{T}_6| &= \gamma_s |L\nu i_h^n(\boldsymbol{u}^n, \boldsymbol{v}_h) + {}^{L}/_{\nu} i_h^n(\boldsymbol{u}^n, \boldsymbol{v}_h) + {}^{1}/_{\nu} j_h^n(p^n, q_h)| \\
&\lesssim (\nu + {}^1/_\nu) L^{1/2} i_h^n(\boldsymbol{u}^n, \boldsymbol{u}^n)^{1/2} L^{1/2} i_h^n(\boldsymbol{v}_h, \boldsymbol{v}_h)^{1/2} + j_h^n(p^n, p^n)^{1/2} j_h^n(q_h, q_h)^{1/2} \\
&\lesssim (\nu + {}^1/_\nu) h^m L^{1/2} \|\boldsymbol{u}^n\|_{\boldsymbol{\mathcal{H}}^{m+1}(\mathcal{O}^n_{\delta_h,\mathscr{T}})} \|\boldsymbol{v}_h\|_{\boldsymbol{\mathcal{H}}^1(\mathcal{O}^n_{\delta_h,\mathscr{T}})} + h^m \|p^n\|_{\mathcal{H}^m(\mathcal{O}^n_{\delta_h,\mathscr{T}})} \|q_h\|_{\mathcal{O}^n_{\delta_h,\mathscr{T}}} \\
&\lesssim (\nu + {}^1/_\nu) h^m L^{1/2} \|\boldsymbol{u}^n\|_{\boldsymbol{\mathcal{H}}^{m+1}(\Omega^n)} |||\boldsymbol{v}_h|||_{*,n} + h^m \|p^n\|_{\mathcal{H}^m(\Omega^n)} |||q_h|||_{*,n}.
\end{aligned} \tag{5.37}$$

Combining estimates (5.27), (5.28), (5.32), (5.34), (5.35) and (5.36) then gives the desired result. □

5.6 *Error estimates*

We define $\boldsymbol{u}_I^n := \mathcal{I}^* \boldsymbol{u}^n$ and $p_I^n := \mathcal{I}^* p^n$. We then split the velocity error $\mathbb{E}^n$ and the pressure $\mathbb{D}^n$ each into an interpolation and discretization error

$$\begin{aligned}
\mathbb{E}^n &= (\boldsymbol{u}^n - \boldsymbol{u}_I^n) + (\boldsymbol{u}_I^n - \boldsymbol{u}_h^n) =: \boldsymbol{\eta}^n + \mathbf{e}_h^n \\
\mathbb{D}^n &= (p^n - p_I^n) + (p_I^n - p_h^n) \;=: \zeta^n + \mathrm{d}_h^n.
\end{aligned}$$

Inserting this into the error equation (5.27) and rearranging terms then yields

$$\begin{aligned}
\int_{\Omega_h^n} \frac{\mathbf{e}_h^n - \mathbf{e}_h^{n-1}}{\Delta t} \cdot \boldsymbol{v}_h \,\mathrm{d}\boldsymbol{x} + a_n^h(\mathbf{e}_h^n, \boldsymbol{v}_h) + b_h^n(\mathrm{d}_h^n, \boldsymbol{v}_h) + b_h^n(q_h, \mathbf{e}_h^n) + s_h^n((\mathbf{e}_h^n, \mathrm{d}_h^n), (\boldsymbol{v}_h, q_h)) \\
= \mathfrak{E}_c^n(\boldsymbol{v}_h, q_h) + \mathfrak{E}_I^n(\boldsymbol{v}_h, q_h)
\end{aligned} \tag{5.38}$$

with

$$\mathfrak{E}_I^n(\boldsymbol{v}_h, q_h) = -\int_{\Omega_h^n} \frac{\boldsymbol{\eta}^n - \boldsymbol{\eta}^{n-1}}{\Delta t} \cdot \boldsymbol{v}_h \,\mathrm{d}\boldsymbol{x} - a_n^h(\boldsymbol{\eta}^n, \boldsymbol{v}_h) - b_h^n(\zeta^n, \boldsymbol{v}_h) - b_h^n(q_h, \boldsymbol{\eta}^n) - s_h^n((\boldsymbol{\eta}^n, \zeta^n), (\boldsymbol{v}_h, q_h)).$$

For the interpolation error component we can prove the following estimate.

LEMMA 5.15 Assume for the velocity that $\boldsymbol{u} \in \boldsymbol{\mathcal{L}}^\infty(0, T; \boldsymbol{\mathcal{H}}^{m+1}(\Omega(t)))$, $\boldsymbol{u}_t \in \boldsymbol{\mathcal{L}}^\infty(0, T; \boldsymbol{\mathcal{H}}^m(\Omega(t)))$ and for the pressure that $p \in \mathcal{L}^\infty(0, T; \mathcal{H}^m(\Omega(t)))$. We can then bound the interpolation error term by

$$|\mathfrak{E}_I^n(\boldsymbol{v}_h, q_h)| \lesssim \frac{h^m L^{1/2}}{\nu} R_{I,1}(\boldsymbol{u}, p) |||\boldsymbol{v}_h|||_{*,n} + h^m R_{I,2}(\boldsymbol{u}, p) |||q_h|||_{*,n},$$

with

$$R_{I,1}(\boldsymbol{u},p) = \sup_{t\in[0,T]} \Big(\|\boldsymbol{u}\|_{\boldsymbol{\mathcal{H}}^{m+1}(\Omega(t))} + \|\boldsymbol{u}_t\|_{\boldsymbol{\mathcal{H}}^{m}(\Omega(t))} + \|p\|_{\mathcal{H}^{m}(\Omega(t))} \Big)$$

and

$$R_{I,2}(\boldsymbol{u},p) = \sup_{t\in[0,T]} \Big(\|\boldsymbol{u}\|_{\boldsymbol{\mathcal{H}}^{m+1}(\Omega(t))} + \|p\|_{\mathcal{H}^{m}(\Omega(t))} \Big).$$

Proof. We split the interpolation error terms into five different parts $\mathfrak{E}_I^n(\boldsymbol{v}_h, q_h) = \mathfrak{T}_7 + \mathfrak{T}_8 + \mathfrak{T}_9 + \mathfrak{T}_{10} + \mathfrak{T}_{11}$. These are the time-derivative term, the diffusion bilinear form, the pressure coupling term, the divergence constraint and ghost-penalty operator, respectively. As in Lemma 5.14 we deal with each constituent term separately.

For the time-derivative contribution $\mathfrak{T}_7$ we have from Lehrenfeld & Olshanskii (2019, Lemma 5.12) that

$$|\mathfrak{T}_7| = \Big| \int_{\Omega_h^n} \frac{\boldsymbol{\eta}^n - \boldsymbol{\eta}^{n-1}}{\Delta t} \cdot \boldsymbol{v}_h \mathrm{d}\boldsymbol{x} \Big| \lesssim h^m \sup_{t\in[0,T]} \big(\|\boldsymbol{u}\|_{\boldsymbol{\mathcal{H}}^{m+1}(\Omega(t))} + \|\boldsymbol{u}_t\|_{\boldsymbol{\mathcal{H}}^{m}(\Omega(t))} \big) \|\boldsymbol{v}_h\|_{\Omega_h^n}.$$

For the diffusion term $\mathfrak{T}_8$ we use the continuity result (5.8) and Lemma 5.2 for the interpolation term and (5.4) for the test function, which gives

$$|\mathfrak{T}_8| = |-a_h^n(\boldsymbol{\eta}^n, \boldsymbol{v}_h)| \lesssim |||\boldsymbol{\eta}^n|||_n |||\boldsymbol{v}_h|||_n \lesssim h^m \|\boldsymbol{u}^n\|_{\boldsymbol{\mathcal{H}}^{m+1}(\Omega^n)} |||\boldsymbol{v}_h|||_{*,n}.$$

Using the same technique we can estimate the pressure and divergence bilinear forms as

$$\begin{aligned} |\mathfrak{T}_9| &= |-b_h^n(\zeta^n, \boldsymbol{v}_h)| \lesssim h^m \|p^n\|_{\mathcal{H}^m(\Omega^n)} |||\boldsymbol{v}_h|||_{*,n} \\ |\mathfrak{T}_{10}| &= |-b_h^n(q_h, \boldsymbol{\eta}^n)| \lesssim h^m \|\boldsymbol{u}^n\|_{\boldsymbol{\mathcal{H}}^{m+1}(\Omega^n)} |||q_h|||_{*,n}. \end{aligned}$$

For the ghost-penalty term $\mathfrak{T}_{11}$ (see also Lehrenfeld & Olshanskii, 2019, Lemma 5.12) we use the Cauchy–Schwarz inequality and Lemma 4.1 with (3.3a)

$$\begin{aligned} |\mathfrak{T}_{11}| = |s_h^n((\boldsymbol{\eta}^n,\zeta^n),(\boldsymbol{v}_h,q_h))| &\lesssim (\nu + 1/\nu) L^{1/2} i_h^n(\boldsymbol{\eta}^n,\boldsymbol{\eta}^n)^{1/2} L^{1/2} i_h^n(\boldsymbol{v}_h,\boldsymbol{v}_h)^{1/2} + j_h^n(\zeta^n,\zeta^n)^{1/2} j_h^n(q_h,q_h)^{1/2} \\ &\lesssim (\nu + 1/\nu) h^m L^{1/2} \|\boldsymbol{u}^n\|_{\boldsymbol{\mathcal{H}}^{m+1}(\mathcal{O}^n_{\delta_h,\mathscr{T}})} \|\boldsymbol{v}_h\|_{\mathcal{O}^n_{\delta_h,\mathscr{T}}} + h^m \|p^n\|_{\mathcal{H}^m(\mathcal{O}^n_{\delta_h,\mathscr{T}})} \|q_h\|_{\mathcal{O}^n_{\delta_h,\mathscr{T}}} \\ &\lesssim (\nu + 1/\nu) h^m L^{1/2} \|\boldsymbol{u}^n\|_{\boldsymbol{\mathcal{H}}^{m+1}(\Omega^n)} |||\boldsymbol{v}_h|||_{*,n} + h^m \|p^n\|_{\mathcal{H}^m(\Omega^n)} |||q_h|||_{*,n}. \end{aligned}$$

□

THEOREM 5.16 For sufficiently small Δt and h the velocity error can be bounded by

$$\|\mathbb{E}^n\|^2_{\Omega_h^n} + \sum_{k=1}^{n}\left\{\|\mathbb{E}^k - \mathbb{E}^{k-1}\|^2_{\Omega_h^k} + \Delta t\big[\nu c_{L5.5}|||\mathbb{E}^k|||^2_{*,k} + \frac{L}{\nu} i_h^k(\mathbb{E}^k,\mathbb{E}^k)\big]\right\}$$
$$\leq \exp((c_{T5.16\mathrm{a}}/\nu)t_n)\left[\Delta t\sum_{k=1}^{n} c_{T5.16\mathrm{b}}\Big[\Delta t^2 + h^{2q} + \frac{h^{2m}L}{\nu^2} + \frac{1}{\Delta t}\left(h^{2q} + \frac{h^{2m}}{\nu^2}\right)\Big]R(\boldsymbol{u},p,\boldsymbol{f})\right]$$

with $R(\boldsymbol{u},p,\boldsymbol{f}) = \sup_{t\in[0,T]}(\|\boldsymbol{u}\|^2_{\boldsymbol{\mathcal{H}}^{m+1}(\Omega(t))} + \|\boldsymbol{u}_t\|^2_{\boldsymbol{\mathcal{H}}^{m}(\Omega(t))} + \|p\|^2_{\mathcal{H}^{m}(\Omega(t))}) + \|\boldsymbol{u}\|^2_{\boldsymbol{\mathcal{W}}^{2,\infty}(\mathcal{Q})} + \|\boldsymbol{f}\|^2_{\boldsymbol{\mathcal{H}}^1(\Omega^n)}$ and constants $c_{T5.16}$ independent of Δt, n and h.

For the pressure we have the bound

$$\Delta t^2\sum_{k=1}^{n}|||\mathbb{D}^k|||^2_{*,k} \lesssim \Delta t\sum_{k=1}^{n-1}\frac{1}{\nu}\|\mathbb{E}^k\|^2_{\Omega_h^k} + \Delta t\sum_{k=1}^{n} c\Big[\Delta t^2 + h^{2q} + \frac{h^{2m}L}{\nu^2} + \frac{1}{\Delta t}\Big(h^{2q} + \frac{h^{2m}}{\nu^2}\Big)\Big]R(\boldsymbol{u},p,\boldsymbol{f}).$$

Proof. We prove the result for the discretization error, since the result then immediately follows by optimal interpolation properties. We start with the velocity estimate. Similar to the stability proof, for $n=k$, we test the error equation (37) with the test-function $(\boldsymbol{v}_h, q_h) = 2\Delta t(\mathbf{e}_h^k, -\mathrm{d}_h^k)$ and use the identity (5.13) to get

$$\big\|\mathbf{e}_h^k\big\|^2_{\Omega_n^k} + \big\|\mathbf{e}_h^k - \mathbf{e}_h^{k-1}\big\|^2_{\Omega_h^k} + 2\Delta t\big(a_h^k + \nu L i_h^k\big)\big(\mathbf{e}_h^k,\mathbf{e}_h^k\big) + {}^{2L\Delta t}/_{\nu}\, i_h^k\big(\mathbf{e}_h^k,\mathbf{e}_h^k\big) + {}^{2\Delta t}/_{\nu}\, j_h^k\big(\mathrm{d}_h^k,\mathrm{d}_h^k\big)$$
$$= 2\Delta t\big(\mathfrak{E}_c^k + \mathfrak{E}_I^k\big)\big(\mathbf{e}_h^k, -\mathrm{d}_h^k\big) + \big\|\mathbf{e}_h^{k-1}\big\|^2_{\Omega_h^k}.$$

Using the coercivity result Lemma 5.5 and (5.16) we get (with the appropriate choice of ε) that

$$\|\mathbf{e}_h^k\|^2_{\Omega_n^k} + \|\mathbf{e}_h^k - \mathbf{e}_h^{k-1}\|^2_{\Omega_h^k} + 2\Delta t c_{L5.5}|||\mathbf{e}_h^k|||^2_{*,k} + \Delta t\frac{2L}{\nu} i_h^k\big(\mathbf{e}_h^k,\mathbf{e}_h^k\big) + \Delta t\frac{2}{\nu} j_h^k\big(\mathrm{d}_h^k,\mathrm{d}_h^k\big)$$
$$\leq \left(1 + \frac{\overline{c}}{\nu}\Delta t\right)\|\mathbf{e}_h^{k-1}\|^2_{\Omega_h^{k-1}} + \Delta t\frac{\nu c_{L5.5}}{2}|||\mathbf{e}_h^{k-1}|||^2_{*,k-1} + \Delta t\frac{c' h^2}{\nu} L i_h^{k-1}\big(\mathbf{e}_h^{k-1},\mathbf{e}_h^{k-1}\big)$$
$$+ 2\Delta t\big(|\mathfrak{E}_c^k| + |\mathfrak{E}_I^k|\big)\big(\mathbf{e}_h^k,\mathrm{d}_h^k\big).$$

Applying the weighted Young inequality to Lemma 5.14 and Lemma 5.15 then gives

$$\big|\mathfrak{E}_c^k(\mathbf{e}_h^k,\mathrm{d}_h^k) + \mathfrak{E}_I^k(\mathbf{e}_h^k,\mathrm{d}_h^k)\big|$$
$$\leq \frac{1}{\varepsilon_1}c\left(\Delta t^2 + h^{2q} + \frac{h^{2m}L}{\nu^2}\right)R(\boldsymbol{u},p,\boldsymbol{f}) + \varepsilon_1|||\mathbf{e}_h^k|||^2_{*,k} + \frac{1}{\varepsilon_2}c\left(h^{2q} + \frac{h^{2m}}{\nu^2}\right)R'(\boldsymbol{u},p) + \varepsilon_2|||\mathrm{d}_h^k|||^2_{*,k}$$

with

$$R'(\boldsymbol{u},p) = \sup_{t\in[0,T]} \left(\|\boldsymbol{u}(t)\|^2_{\boldsymbol{\mathcal{H}}^{m+1}(\Omega(t))} + \|p(t)\|^2_{\mathcal{H}^m(\Omega(t))}\right).$$

Now we choose $\varepsilon_1 = \nu c_{L5.5}/4$ and $\varepsilon_2 = \Delta t\beta^2/4c_Y c^2_{P,h}$. With the constant $c_Y > 0$ to be specified later. Inserting these bounds on the consistency and interpolation estimates into the above inequality, and summing over $k = 1,\dots,n$ and using $\mathbf{e}_h^0 = \mathbf{0}$ gives

$$\begin{aligned}
\|\mathbf{e}_h^n\|^2_{\Omega_h^k} + \sum_{k=1}^n \|\mathbf{e}_h^k - \mathbf{e}_h^{k-1}\|^2_{\Omega_h^k} + \Delta t \sum_{k=1}^n \left[\nu c_{L5.5} |||\mathbf{e}_h^k|||^2_{*,k} + \frac{L}{\nu} i_h^k(\mathbf{e}_h^k,\mathbf{e}_h^k)\right] + \Delta t \sum_{k=1}^n \frac{2}{\nu} j_h^k(\mathrm{d}_h^k,\mathrm{d}_h^k) \\
\leq \Delta t \sum_{k=1}^{n-1} \frac{\bar{c}}{\nu} \|\mathbf{e}_h^k\|^2_{\Omega_h^k} + \Delta t^2 \sum_{k=1}^{2} \frac{\beta^2}{2c_Y c^2_{P,h}} |||\mathrm{d}_h^k|||^2_{*,k} \\
+ \Delta t \sum_{k=1}^n c\left[\Delta t^2 + h^{2q} + \frac{h^{2m}L}{\nu^2} + \frac{1}{\Delta t}\left(h^{2q} + \frac{h^{2m}}{\nu^2}\right)\right] R(\boldsymbol{u},p,\boldsymbol{f}),
\end{aligned} \tag{5.39}$$

under the assumption, that h is sufficiently small, such that $c'h^2 \leq 1$. To complete the velocity estimate we therefore require the pressure estimate.

Rearranging the error equation (37) and using the test-function $q_h = 0$ gives

$$\begin{aligned}
b_h^k(\mathrm{d}_h^k,\boldsymbol{v}_h) &= -(1/\Delta t(\mathbf{e}_h^k - \mathbf{e}_h^{k-1}),\boldsymbol{v}_h)_{\Omega_h^k} - (a_h^k + \nu L i_h^k)(\mathbf{e}_h^k,\boldsymbol{v}_h) - \frac{L}{\nu} i_h^k(\mathbf{e}_h^k,\boldsymbol{v}_h) + (\mathfrak{E}_c^k + \mathfrak{E}_I^k)(\mathbf{e}_h^k,0) \\
&\leq \left[\frac{c_{P,h}}{\Delta t}\|\mathbf{e}_h^k - \mathbf{e}_h^{k-1}\|_{\Omega_h^k} + \nu c_{L5.4} |||\mathbf{e}_h^k|||_{*,k} + \frac{L^{1/2}}{\nu} i_h^k(\mathbf{e}_h^k,\mathbf{e}_h^k)^{1/2}\right. \\
&\quad \left. + \hat{c}\left(\Delta t + h^q + \frac{L^{1/2}h^m}{\nu}\right)(R_{c,1} + R_{I,1})(\boldsymbol{u},p,\boldsymbol{f})\right] |||\boldsymbol{v}_h|||_{*,k},
\end{aligned}$$

where $\hat{c} = c_{L5.14} + c_{L5.14}$. Using the inf-sup result from Lemma 5.6 together with (5.7c) we then have

$$\begin{aligned}
\beta |||\mathrm{d}_h^k|||_{*,k} \leq \frac{c_{P,h}}{\Delta t}\|\mathbf{e}_h^k - \mathbf{e}_h^{k-1}\|_{\Omega_h^k} + \nu c_{L5.4} |||\mathbf{e}_h^k|||_{*,k} + \frac{L^{1/2}}{\nu} i_h^k(\mathbf{e}_h^k,\mathbf{e}_h^k)^{1/2} + (1+\beta) j_h^n(\mathrm{d}_h^k,\mathrm{d}_h^k)^{1/2} \\
+ \hat{c}\left(\Delta t + h^q + \frac{L^{1/2}h^m}{\nu}\right)(R_{c,1} + R_{I,1})(\boldsymbol{u},p,\boldsymbol{f}).
\end{aligned}$$

Squaring this, using Young's inequality to remove the product terms multiplying with Δt^2 and summing over $k = 1, \ldots, n$ we get

$$\Delta t^2 \sum_{k=1}^{n} \frac{\beta^2}{c_{P,h}^2 c_Y} |||\mathrm{d}_h^k|||_{*,k}^2 \leq \sum_{k=1}^{n} \|\mathbf{e}_h^k - \mathbf{e}_h^{k-1}\|_{\Omega_h^k}^2 + \Delta t \sum_{k=1}^{n} \left[\Delta t(\nu^2 c_{L5.5}^2)|||\mathbf{e}_h^k|||_{*,k}^2 + \frac{\Delta t L}{\nu^2} i_h^k(\mathbf{e}_h^k, \mathbf{e}_h^k)\right]$$
$$+ \Delta t \sum_{k=1}^{n} \Delta t(1+\beta)^2 j_h^n(\mathrm{d}_h^k, \mathrm{d}_h^k) + \Delta t \sum_{k=1}^{n} \Delta t \hat{c}^2 \left(\Delta t^2 + h^{2q} + \frac{L h^{2m}}{\nu^2}\right) R(\boldsymbol{u}, p, \boldsymbol{f}) \quad (5.40)$$

where c_Y stems from the estimate $(\sum_{i=1}^n a_i)^2 \leq n \sum_{i=1}^n a_i^2$. We make the technical assumptions that $\Delta t \nu^2 c_{L5.4}^2 \leq \nu c_{L5.4}$ and $\Delta t(1+\beta^2) \leq 2/\nu$. Note that since we are interested in the case of $\nu \ll 1$ these assumptions are not problematic and the inequalities are not sharp. For sufficiently small Δt, that is $\Delta t L/\nu^2 \leq 2L/\nu$, we can then bound the right-hand side of (39) with (38), which proves the error estimate.

The pressure discretization error on the right-hand side of (38) can therefore be bounded by the other terms on the right-hand side of (38). This then gives us the estimate

$$\|\mathbf{e}_h^n\|_{\Omega_h^k}^2 + \sum_{k=1}^{n} \left\{ \|\mathbf{e}_h^k - \mathbf{e}_h^{k-1}\|_{\Omega_h^k}^2 + \Delta t \left[\nu c_{L5.4} |||\mathbf{e}_h^k|||_{*,k}^2 + \frac{L}{\nu} i_h^k(\mathbf{e}_h^k, \mathbf{e}_h^k)\right]\right\}$$
$$\leq \Delta t \sum_{k=1}^{n-1} \frac{2\overline{c}}{\nu} \|\mathbf{e}_h^k\|_{\Omega_h^k}^2 + \Delta t \sum_{k=1}^{n} 2c \left[\Delta t^2 + h^{2q} + \frac{h^{2m} L}{\nu^2} + \frac{1}{\Delta t}\left(h^{2q} + \frac{h^{2m}}{\nu^2}\right)\right] R(\boldsymbol{u}, p, \boldsymbol{f}). \quad (5.41)$$

Applying Gronwall's Lemma then proves the result. □

REMARK 5.17 To be able to get an optimal estimate for the velocity and pressure error from the above proof, which do not depend on negative powers of Δt, we would need an estimate for $1/\Delta t \|\mathbf{e}_h^k - \mathbf{e}_h^{k-1}\|_{\Omega_h^k}^2$, which is independent of negative powers of Δt. Standard approaches to estimate this, such as in Besier & Wollner (2011), do not work here, since the proof requires $\mathbf{e}_h^k - \mathbf{e}_h^{k-1}$ to be weakly divergence free with respect to Q_h^k. An alternative would be to estimate $\left\| \frac{\mathbf{e}_h^k - \mathbf{e}_h^{k-1}}{\Delta t} \right\|_{-1}$. However, standard approaches such as in de Frutos *et al.* (2015) are again not viable due to lack of weak divergence conformity of the solution at two different time steps.

If such an estimate was at hand we would also be able to avoid the negative power of Δt on the right-hand side of both the velocity and pressure estimates.

REMARK 5.18 The choice of $\Delta t \sim h$ would lead to an overall loss of half an order in the energy norm, provided that the spatial error is dominant. However, since this term is the result of lack of full consistency of the method (due to geometry approximation, ghost-penalties and divergence constraint with respect to different spaces for different time steps), we do not expect that this is the major, dominating error part.

REMARK 5.19 It cannot be expected that the above result is sharp, since we have made some very crude estimates to bound (39) with (38).

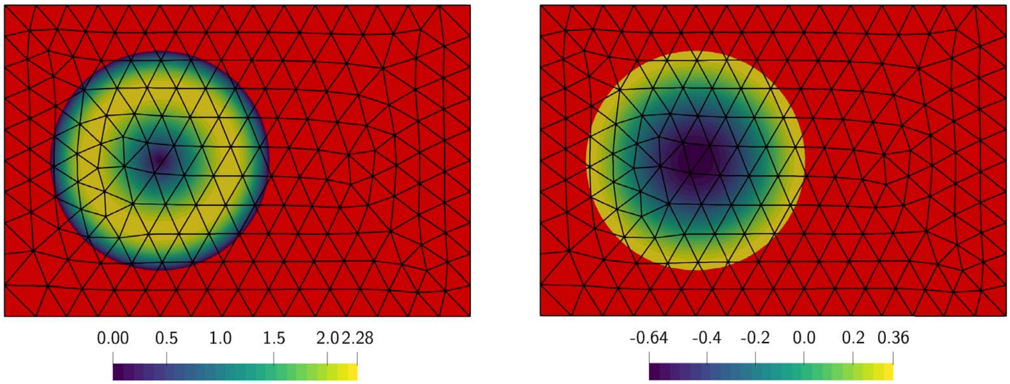

FIG. 2. Velocity magnitude and pressure of the analytical solution at $t = 0$.

REMARK 5.20 (Extension to higher-order BDF schemes). As remarked upon in Burman *et al.* (2019), Lehrenfeld & Olshanskii (2019), the extension to higher oder BDF methods such as BDF2 is relatively unproblematic.

6. Numerical examples

The method has been implemented using `ngsxfem` (Lehrenfeld *et al.*, 2021), an add-on package to the high-order finite-element library `NGSolve/Netgen` (Schöberl, 1997, 2014). The resulting sparse linear systems are solved using the direct solver `Pardiso`, as part of the `Intel MKL` library (Intel, 2019).

Full datasets of the computations shown here, as well as scripts to reproduce the results, can be found online: DOI: 10.5281/zenodo.3647571.

6.1 *General set-up*

As a test case we consider a basic test case with an analytical solution. On the domain $\Omega(t) = \{\boldsymbol{x} \in \mathbb{R}^2 \mid (\boldsymbol{x}_1 - t)^2 + \boldsymbol{x}_2^2 < 1/2\}$ we consider the analytical solution

$$\boldsymbol{u}_{ex}(t) = \begin{pmatrix} 2\pi \boldsymbol{x}_2 \cos(\pi((\boldsymbol{x}_1 - t)^2 + \boldsymbol{x}_2^2)) \\ -2\pi \boldsymbol{x}_1 \cos(\pi((\boldsymbol{x}_1 - t)^2 + \boldsymbol{x}_2^2)) \end{pmatrix} \quad \text{and} \quad p_{ex}(t) = \sin(\pi((\boldsymbol{x}_1 - t)^2 + \boldsymbol{x}_2^2)) - 2/\pi.$$

The velocity $\boldsymbol{u}_{ex}(t)$ then fulfils homogeneous Dirichlet boundary conditions and we have $p_{ex}(t) \in \mathcal{L}_0^2(\Omega_n(t))$. An illustration of the initial solution on the initial background mesh can be seen in Fig. 2. The forcing vector is then chosen accordingly as $\boldsymbol{f}(t) = \partial_t \boldsymbol{u}_{ex}(t) - \nu \Delta \boldsymbol{u}_{ex}(t) + \nabla p_{ex}(t)$.

We then consider the following set-up: the time interval is $[0, 1]$ and the background domain is taken as $\widetilde{\Omega} = (-1, -2) \times (1, 1)$. The maximum interface speed in our time interval is then $w_\infty^n = 1$ and for the strip-width we choose $c_\delta = 1$. Unless otherwise stated we take the Nitsche penalty parameter as $\sigma = 40k^2$. On the mesh we consider the lowest order Taylor–Hood elements, i.e., $k = 2$. However, as the geometry is approximated by a piecewise linear level set function, we have $q = 1$, so that we cannot expect to get the full spatial convergence order from the elements.

To quantify the computational results we will consider the following discrete space–time errors:

$$\|\boldsymbol{u}_h - \boldsymbol{u}\|^2_{\ell^2(\boldsymbol{\mathcal{L}}^2)} := \Delta t \sum_{k=1}^{n} \|\boldsymbol{u}_h - \boldsymbol{u}\|^2_{\boldsymbol{\mathcal{L}}^2(\Omega_h^k)} \qquad \|\boldsymbol{u}_h - \boldsymbol{u}\|^2_{\ell^2(\boldsymbol{\mathcal{H}}^1)} := \Delta t \sum_{k=1}^{n} \|\nabla \boldsymbol{u}_h - \nabla \boldsymbol{u}\|^2_{\boldsymbol{\mathcal{L}}^2(\Omega_h^k)}$$

$$\|p_h - p\|^2_{\ell^2(\boldsymbol{\mathcal{L}}^2)} := \Delta t \sum_{k=1}^{n} \|p_h - p\|^2_{\mathcal{L}^2(\Omega_h^k)}.$$

6.2 *Parameter dependence*

We investigate the robustness of our method with respect to the viscosity ν, the ghost-penalty stabilization parameter γ_s and the extension strip-width, in terms of the number of elements L. For this we take the time-step $\Delta t = 0.05$. The viscosity is taken as $\nu \in \{10^0, 10^{-1}, \dots, 10^{-4}\}$ and the stabilization is taken as $\gamma_s \in \{0.1, 1, \dots, 10^3\}$. To increase the strip-width $L = \lceil \delta_h / h_{max} \rceil$ we take $h_{max} = 0.1, 0.025, 0.0125$, resulting in $L = 1, 2, 4$, respectively.

The results for the $\ell^2(\boldsymbol{\mathcal{L}}^2)$-velocity error of these computations can be seen in Table 1. Here we observe that the method is robust with respect to over-stabilization. We also note that within the considered range the method is also robust with respect to number of elements in the extension strip. The method seems to be particularly robust over a wide range of viscosities. With a decrease of the viscosity by a factor 10^4, the velocity error only increased by a factor of 50 on the coarsest mesh, while on the finer meshes, this increase was even smaller. Furthermore, we see that we have a stable solution for very small ν, where the assumption $\Delta t \sim \nu$ made in Theorem 5.16 does not hold anymore.

REMARK 6.1 In computations, where we extended the pressure into the same exterior domain as the velocity, i.e., $\mathscr{T}^n_{h,\mathcal{S}^+}$, by using ghost penalties based on the same facets $\mathscr{F}^n_{h,\delta_h}$ and using the same ghost-penalty parameter (up to h and ν-scaling) $\gamma_{s,u} = \gamma'_{s,u} = \gamma_{s,p} = L\gamma_s$ lead to qualitatively the same results as the results presented here and in the subsequent sections, only with slightly larger error constants.

6.3 *Convergence study*

To investigate the asymptotic convergence behaviour of the method in both time and space we compute the *experimental order of convergence* in space (eoc_x) and time (eoc_t), based on the errors of two successive refinement levels of the respective variable and the finest refinement level of the other variable. The analysis predicts that spatial error is corrupted by a factor Δt^{-1}. To investigate this numerically we also compute the eoc for one refinement in both space and time (eoc_{xt}).

To study the asymptotic temporal and spatial convergence properties of the analysed method we consider the following set-up. The viscosity is chosen as $\nu = 10^{-2}$ and the ghost-penalty parameter is $\gamma_s = 1$. The initial time step is $\Delta t_0 = 0.1$ and the initial mesh size is $h_0 = 0.2$. We consider a series of uniform refinements by a factor 2 in both time and space, such that $h_{max} = h_0 \cdot 2^{-L_x}$ and $\Delta t = \Delta t_0 \cdot 2^{-L_t}$. The remaining parameters are as described in Section 6.1. In total we make four spatial and eight temporal refinements.

The results for all three discrete space–time norms can be seen in Table 2. With respect to time we see the expected linear convergence ($\text{eoc}_t \approx 1$) in all three considered norms. With respect to space (eoc_x) we see lower than optimal convergence rates, before the temporal error begins to dominate. However, the rates are also higher than the expected rates if the geometry error was dominant. We attribute this to an interplay between the geometry error and the $1/\nu$ scaled consistency error from the ghost-penalties.

TABLE 1 $\ell^2(0,T;\boldsymbol{\mathcal{L}}^2(\Omega(t)))$ *velocity error for the BDF1 method over a range of viscosities and ghost-penalty parameters*

$\nu\downarrow \backslash\gamma_s\rightarrow$	0.1	1	10	100	1000
1	4.0×10^{-2}	4.1×10^{-2}	4.5×10^{-2}	6.3×10^{-2}	1.6×10^{-1}
0.1	1.8×10^{-1}	1.9×10^{-1}	2.3×10^{-1}	4.5×10^{-1}	1.2×10^{0}
0.01	3.7×10^{-1}	4.5×10^{-1}	7.8×10^{-1}	1.4×10^{0}	1.6×10^{0}
0.001	4.2×10^{-1}	6.7×10^{-1}	1.1×10^{0}	1.3×10^{0}	1.3×10^{0}
0.0001	2.1×10^{0}	3.6×10^{0}	4.1×10^{0}	4.3×10^{0}	4.3×10^{0}

(a) $h_{max}=0.1$ and $\Delta t=0.05$ and a resulting strip width of $L=1$

$\nu\downarrow \backslash\gamma_s\rightarrow$	0.1	1	10	100	1000
1	2.7×10^{-2}	2.7×10^{-2}	2.7×10^{-2}	2.7×10^{-2}	2.7×10^{-2}
0.1	1.7×10^{-1}	1.7×10^{-1}	1.7×10^{-1}	1.7×10^{-1}	1.9×10^{-1}
0.01	3.3×10^{-1}	3.3×10^{-1}	3.4×10^{-1}	3.8×10^{-1}	6.5×10^{-1}
0.001	3.7×10^{-1}	3.7×10^{-1}	4.2×10^{-1}	6.7×10^{-1}	8.9×10^{-1}
0.0001	3.5×10^{-1}	3.5×10^{-1}	4.4×10^{-1}	5.6×10^{-1}	5.7×10^{-1}

(b) $h_{max}=0.025$ and $\Delta t=0.05$ and a resulting strip width of $L=2$

$\nu\downarrow \backslash\gamma_s$	0.1	1	10	100	1000
1	2.6×10^{-2}	2.6×10^{-2}	2.6×10^{-2}	2.6×10^{-2}	2.6×10^{-2}
0.1	1.7×10^{-1}	1.7×10^{-1}	1.7×10^{-1}	1.7×10^{-1}	1.7×10^{-1}
0.01	3.3×10^{-1}	3.3×10^{-1}	3.3×10^{-1}	3.4×10^{-1}	4.0×10^{-1}
0.001	3.7×10^{-1}	3.7×10^{-1}	3.7×10^{-1}	4.5×10^{-1}	7.0×10^{-1}
0.0001	3.6×10^{-1}	3.7×10^{-1}	3.9×10^{-1}	4.8×10^{-1}	5.4×10^{-1}

(c) $h_{max}=0.0125$ and $\Delta t=0.05$ and a resulting strip width of $L=4$

With respect to space (eoc_x) we observe at least second-order convergence in all norms. This is as good as the best approximation error for the $\ell^2(\mathcal{L}^2)$-norm of the pressure and the $\ell^2(\boldsymbol{\mathcal{H}}^2)$-norm of the velocity error, while for the $\ell^2(\boldsymbol{\mathcal{L}}^2)$ velocity error we see a convergence rate that is worse than its approximation error. This however is to be expected if the geometry errors with $q=1$ are taken into consideration.

To check whether the factor $(h^{2q}+h^{2m})/\Delta t$ is observable we consider joint refinement of both time and space with $L_t=L_x+4$ for which the theory predicts a loss half an order of convergence. However, in Table 2, we see that $\mathrm{eox}_{tx}\approx\mathrm{eox}_x$. This suggests that this part of the analysis is indeed not sharp, as discussed and expected above.

For the $\ell^2(\mathcal{L}^2)$-pressure error we observe that the experimental order of convergence in space is higher than expected. This suggests that the velocity error on the right-hand side of the pressure estimate is dominating term here.

TABLE 2 *Mesh-size and time-step convergence for the BDF1 method with* $\nu = 10^{-2}$

$L_t \downarrow \backslash L_x \rightarrow$	0	1	2	3	4	eoc_t
0	1.3×10^{0}	7.4×10^{-1}	6.6×10^{-1}	6.5×10^{-1}	6.5×10^{-1}	
1	1.0×10^{0}	4.4×10^{-1}	3.4×10^{-1}	3.3×10^{-1}	3.3×10^{-1}	0.99
2	8.2×10^{-1}	2.8×10^{-1}	1.8×10^{-1}	1.7×10^{-1}	1.7×10^{-1}	0.99
3	7.3×10^{-1}	1.9×10^{-1}	9.9×10^{-2}	8.6×10^{-2}	8.4×10^{-2}	0.99
4	6.9×10^{-1}	1.6×10^{-1}	5.7×10^{-2}	4.4×10^{-2}	4.2×10^{-2}	0.99
5	6.7×10^{-1}	1.4×10^{-1}	3.7×10^{-2}	2.3×10^{-2}	2.1×10^{-2}	0.99
6	6.6×10^{-1}	1.3×10^{-1}	2.8×10^{-2}	1.2×10^{-2}	1.1×10^{-2}	0.98
7	6.5×10^{-1}	1.3×10^{-1}	2.3×10^{-2}	7.2×10^{-3}	5.5×10^{-3}	0.97
8	6.5×10^{-1}	1.2×10^{-1}	2.1×10^{-2}	4.7×10^{-3}	2.9×10^{-3}	0.94
eoc_x	–	2.39	2.53	2.19	0.72	
eoc_{xt}	–	2.31	2.32	1.95	1.33	

(a) $\ell^2(0,T;\mathcal{L}^2(\Omega(t)))$ velocity error

$L_t \downarrow \backslash L_x \rightarrow$	0	1	2	3	4	eoc_t
0	8.9×10^{0}	5.8×10^{0}	5.4×10^{0}	5.6×10^{0}	6.3×10^{0}	
1	7.9×10^{0}	4.0×10^{0}	3.2×10^{0}	3.2×10^{0}	3.4×10^{0}	0.90
2	6.9×10^{0}	2.8×10^{0}	1.9×10^{0}	1.8×10^{0}	1.9×10^{0}	0.83
3	6.5×10^{0}	2.3×10^{0}	1.1×10^{0}	1.0×10^{0}	1.0×10^{0}	0.87
4	6.3×10^{0}	2.1×10^{0}	7.6×10^{-1}	5.5×10^{-1}	5.5×10^{-1}	0.91
5	6.2×10^{0}	2.0×10^{0}	5.9×10^{-1}	3.0×10^{-1}	2.9×10^{-1}	0.94
6	6.1×10^{0}	2.0×10^{0}	5.3×10^{-1}	1.8×10^{-1}	1.5×10^{-1}	0.96
7	6.1×10^{0}	1.9×10^{0}	5.0×10^{-1}	1.2×10^{-1}	7.6×10^{-2}	0.96
8	6.1×10^{0}	1.9×10^{0}	4.9×10^{-1}	1.0×10^{-1}	4.0×10^{-2}	0.93
eoc_x	–	1.65	1.97	2.27	1.36	
eoc_{xt}	–	1.65	1.92	2.09	1.63	

(b) $\ell^2(0,T;\mathcal{H}^1(\Omega(t)))$ velocity error

$L_t \downarrow \backslash L_x \rightarrow$	0	1	2	3	4	eoc_t
0	7.3×10^{-1}	4.4×10^{-1}	4.1×10^{-1}	4.3×10^{-1}	4.2×10^{-1}	
1	5.9×10^{-1}	2.6×10^{-1}	2.0×10^{-1}	2.0×10^{-1}	2.0×10^{-1}	1.08
2	4.9×10^{-1}	1.7×10^{-1}	1.1×10^{-1}	9.8×10^{-2}	9.7×10^{-2}	1.06
3	4.4×10^{-1}	1.2×10^{-1}	5.9×10^{-2}	5.0×10^{-2}	4.8×10^{-2}	1.01
4	4.3×10^{-1}	9.7×10^{-2}	3.5×10^{-2}	2.5×10^{-2}	2.4×10^{-2}	1.00
5	4.3×10^{-1}	8.7×10^{-2}	2.3×10^{-2}	1.3×10^{-2}	1.2×10^{-2}	0.99
6	4.5×10^{-1}	8.3×10^{-2}	1.8×10^{-2}	7.4×10^{-3}	6.1×10^{-3}	0.98
7	5.0×10^{-1}	8.3×10^{-2}	1.5×10^{-2}	4.5×10^{-3}	3.2×10^{-3}	0.96
8	5.8×10^{-1}	8.7×10^{-2}	1.5×10^{-2}	3.1×10^{-3}	1.7×10^{-3}	0.92
eoc_x	–	2.75	2.57	2.25	0.87	
eoc_{xt}	–	2.30	2.28	1.99	1.42	

(c) $\ell^2(0,T;\mathcal{L}^2(\Omega(t)))$ pressure error

6.4 *Extension to higher order*

6.4.1 *BDF2 time discretization.* As an extension to the presented method we consider the BDF2 formula to discretize the time derivative. To ensure that the appropriate solution history is available on the necessary elements we increase the extension strip with the choice $\delta_h = 2c_\delta w_n^\infty \Delta t$.

We investigate the convergence properties in both time and space. To this end we take the same basic set up as in Section 6.3. However, we take $L_x = 0, \dots, 5$ and $L_t = 0, \dots, 7$. The results from these computations can be seen in Table 3.

We observe that with $L_t = 7$ the spatial error is dominant on all meshes in all three norms and that eoc_x similar to the BDF1 case.

With respect to time we see second order of convergence ($\mathrm{eoc}_t \approx 2$), while the temporal error is dominant. There are also some stability issues for large time steps and large $L = 16, 32$. However, these results are outside the time-step/viscosity range covered by our theory.

6.4.2 *Higher-order spatial convergence.* As we have seen in the theory and some of the numerical results of the previous section the piecewise linear level set approach leads to a loss in the maximal spatial convergence rate of the velocity. A simple and effective—though not very efficient—way to hide the geometrical error and reveal the underling discretization error is the approximation of the geometry based on a piecewise linear level set after s subdivisions of cut elements. As the resulting geometry approximation order is then of order $\mathcal{O}\big((\frac{h}{2^s})^2\big)$, the drawback of this approach is a nonoptimal scaling for $h \to 0$, since s must increase to balance the discretization error on fine meshes.

To balance the geometry error with the discretization error we take $s = \mathcal{O}\big(\log_2(1/h)\big)$ yielding an effective geometry approximation of $\mathcal{O}\big(h^{q+1}\big)$ with $q = 3$. Let us stress that the purpose of this 'trick' is to hide the geometry error and reveal the underlying remaining discretization errors, and is not meant as a solution to the problem of approximating unfitted geometries in general.

Using the same set-up as in Section 6.4.1 and the BDF2 formula to discretize the time derivative, such that the spatial error is dominant for larger time steps, we compute our test problem over a series of uniformly refined meshes. The time step is chosen as $\Delta t = 0.1 \cdot 2^{-8}$, and we consider Taylor–Hood elements with $k = 2$ and $k = 3$.

The results of these computations can be seen in Fig. 3. Here we can see that we have recovered optimal order of convergence in both velocity norms. We also note that the pressure error converges as before, at an order higher than expected.

7. Conclusions and open problems

Conclusion. We have presented, analysed and implemented a fully Eulerian, inf-sup stable, unfitted FEM for the time-dependent Stokes problem on evolving domains. This followed the previous work in Lehrenfeld & Olshanskii (2019) for convection–diffusion problems, and Burman *et al.* (2019) for the time-dependent Stokes problem using equal-order, pressure-stabilized elements. The method is simple to implement in existing unfitted finite element libraries, since all operators are standard in unfitted finite elements.

In the analysis we have seen that the geometrical consistency error, introduced by integrating over discrete, approximated domains Ω_h^n, plays a major role and causes additional coupling between the velocity and pressure errors, which is nonstandard. Furthermore, since the time derivative approximation term $\frac{1}{\Delta t}(\boldsymbol{u}_h^n - \boldsymbol{u}_h^{n-1})$ is not weakly divergence free with respect to the pressure space Q_h^n, we obtained error estimates that are dependent on inverse powers of Δt. Fortunately, this dependence on Δt^{-1} was

TABLE 3 *Mesh-size and time-step convergence for the BDF2 method with* $\nu = 10^{-2}$

$L_t \downarrow \backslash L_x \rightarrow$	0	1	2	3	4	5	eoc_t
0	1.4×10^{0}	5.7×10^{-1}	2.4×10^{-1}	10.0×10^{-2}	1.2×10^{-1}	1.7×10^{0}	
1	1.1×10^{0}	3.0×10^{-1}	1.1×10^{-1}	3.5×10^{-2}	1.9×10^{-2}	2.4×10^{-1}	2.80
2	9.1×10^{-1}	2.1×10^{-1}	4.9×10^{-2}	1.3×10^{-2}	4.6×10^{-3}	4.0×10^{-3}	5.90
3	7.6×10^{-1}	1.6×10^{-1}	3.3×10^{-2}	5.8×10^{-3}	1.4×10^{-3}	9.4×10^{-4}	2.10
4	7.0×10^{-1}	1.4×10^{-1}	2.6×10^{-2}	4.2×10^{-3}	5.9×10^{-4}	2.4×10^{-4}	1.99
5	6.7×10^{-1}	1.3×10^{-1}	2.2×10^{-2}	3.2×10^{-3}	4.5×10^{-4}	8.3×10^{-5}	1.50
6	6.6×10^{-1}	1.3×10^{-1}	2.1×10^{-2}	2.8×10^{-3}	3.7×10^{-4}	6.4×10^{-5}	0.37
7	6.5×10^{-1}	1.2×10^{-1}	2.0×10^{-2}	2.7×10^{-3}	3.4×10^{-4}	6.0×10^{-5}	0.10
eoc_x	–	2.39	2.61	2.94	2.96	2.51	

(a) $\ell^2(0,T;\boldsymbol{\mathcal{L}}^2(\Omega(t)))$ velocity error

$L_t \downarrow \backslash L_x \rightarrow$	0	1	2	3	4	5	eoc_t
0	9.2×10^{0}	5.0×10^{0}	2.7×10^{0}	1.3×10^{0}	2.6×10^{0}	4.3×10^{1}	
1	8.2×10^{0}	3.3×10^{0}	1.6×10^{0}	6.0×10^{-1}	2.6×10^{-1}	1.0×10^{1}	2.03
2	7.5×10^{0}	2.7×10^{0}	9.0×10^{-1}	3.1×10^{-1}	9.5×10^{-2}	5.2×10^{-2}	7.66
3	6.7×10^{0}	2.3×10^{0}	7.0×10^{-1}	1.6×10^{-1}	4.5×10^{-2}	1.5×10^{-2}	1.79
4	6.4×10^{0}	2.1×10^{0}	5.9×10^{-1}	1.3×10^{-1}	2.2×10^{-2}	5.9×10^{-3}	1.36
5	6.2×10^{0}	2.0×10^{0}	5.3×10^{-1}	1.1×10^{-1}	1.9×10^{-2}	2.7×10^{-3}	1.10
6	6.1×10^{0}	2.0×10^{0}	5.1×10^{-1}	9.7×10^{-2}	1.5×10^{-2}	2.3×10^{-3}	0.24
7	6.1×10^{0}	1.9×10^{0}	5.0×10^{-1}	9.4×10^{-2}	1.4×10^{-2}	1.9×10^{-3}	0.29
eoc_x	–	1.65	1.97	2.41	2.79	2.83	

(b) $\ell^2(0,T;\boldsymbol{\mathcal{H}}^1(\Omega(t)))$ velocity error

$L_t \downarrow \backslash L_x \rightarrow$	0	1	2	3	4	5	eoc_t
0	8.2×10^{-1}	3.8×10^{-1}	2.2×10^{-1}	1.5×10^{-1}	3.5×10^{-1}	4.0×10^{0}	
1	6.6×10^{-1}	1.6×10^{-1}	6.8×10^{-2}	4.5×10^{-2}	4.1×10^{-2}	9.6×10^{-1}	2.06
2	5.6×10^{-1}	1.2×10^{-1}	2.3×10^{-2}	1.1×10^{-2}	1.1×10^{-2}	1.1×10^{-2}	6.51
3	4.8×10^{-1}	9.7×10^{-2}	1.9×10^{-2}	2.5×10^{-3}	2.7×10^{-3}	2.8×10^{-3}	1.89
4	4.6×10^{-1}	8.7×10^{-2}	1.6×10^{-2}	2.3×10^{-3}	5.1×10^{-4}	6.8×10^{-4}	2.05
5	4.8×10^{-1}	8.4×10^{-2}	1.4×10^{-2}	2.0×10^{-3}	2.6×10^{-4}	1.5×10^{-4}	2.22
6	5.3×10^{-1}	8.5×10^{-2}	1.4×10^{-2}	1.9×10^{-3}	2.5×10^{-4}	4.3×10^{-5}	1.76
7	6.3×10^{-1}	9.0×10^{-2}	1.4×10^{-2}	1.8×10^{-3}	2.5×10^{-4}	4.1×10^{-5}	0.07
eoc_x	–	2.80	2.67	2.95	2.89	2.58	

(c) $\ell^2(0,T;\mathcal{L}^2(\Omega(t)))$ pressure error

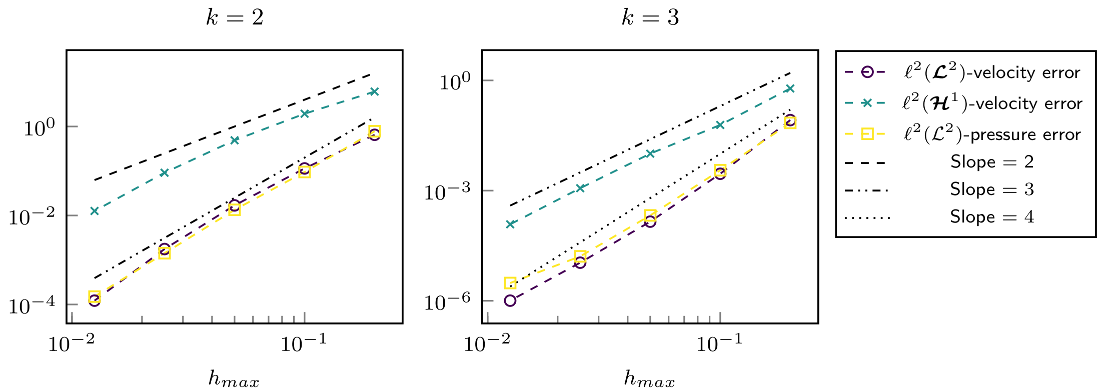

FIG. 3. Results with $k = 2, 3$ using subdivisions for better approximation of the domain boundary.

not observable in our numerical results, suggesting that an estimate of $\|\frac{1}{\Delta t}(\boldsymbol{u}_h^n - \boldsymbol{u}_h^{n-1})\|_{-1}$ independent (of negative powers) of Δt should hold.

In our numerical experiments we have also seen that the geometrical error—if low order approximations are used—can indeed be a dominating factor in the final error, corrupting the optimal convergence rate of the $\mathbb{P}^2/\mathbb{P}^1$ finite element pair. We used a simple, but not efficient, approach for avoiding this in the considered test cases for both $\mathbb{P}^2/\mathbb{P}^1$ and $\mathbb{P}^3/\mathbb{P}^2$ elements.

Open problems. Let us now discuss some issues where further refinement of the method and analysis seem to be of some benefit.

As mentioned above it seems that the term $\|\frac{1}{\Delta t}(\boldsymbol{u}_h^n - \boldsymbol{u}_h^{n-1})\|_{-1}$ is independent of Δt^{-1} for $\boldsymbol{u}_h^{n-1}$ for which we have $b_h^n(q_h, \boldsymbol{u}_h^{n-1}) \neq 0$ for some $q_h \in Q_h^n$. It will be interesting to fix this issue either by enhancing the analysis or modifying the discrete scheme.

Moreover, even in cases where the partial differential equation solution conserves the total momentum, i.e., for suitable boundary conditions and r.h.s. forcings, this will in general not hold true for the discrete solution due to the extension mechanism in the scheme. It is hence a topic of future research to find conservative variants of the scheme presented here, which are at the same time at least second-order accurate.

The exponential growth in the stability estimate, and hence also in the error estimate, is due to a straight-forward application of the Gronwall lemma. However, in the case of velocity fields that drive the domain motion that are divergence free, it is to be expected that an estimate of only linear growth could be achieved. We left this open for future research.

In Section 6.4.2 we have shown that it is possible to recover the optimal order of convergence for the Taylor–Hood finite element pair if sufficient computational effort is put on the geometry approximation. However, the subdivision strategy used here is limited in its application, due to the large number of subdivisions needed after several global mesh refinements and for higher order elements. One approach to efficiently obtain higher order geometry approximations for level set domains has been introduced in Lehrenfeld (2016) for *stationary* domains. That approach relies on a slight local deformations of the mesh, depending on the level set function. For unsteady problems, the corresponding mesh becomes time dependent for which efficient and accurate transfer operations are needed from one mesh to the other. This will be discussed in a forthcoming paper.

Funding

Deutsche Forschungsgemeinschaft (German Research Foundation—314838170, GRK 2297 MathCoRe to H.v.W. and T.R.); Federal Ministry of Education and Research of Germany (project number 05M16NMA to T.R.); Deutsche Forschungsgemeinschaft (German Research Foundation, within the project 'LE 3726/1-1' to C.L.).

References

Ambrosi, D., Quarteroni, A. & Rozza, G., eds. (2012) *Modeling of Physiological Flows*, vol. **5**. Modeling, Simulation and Applications. Milan: Springer. doi: 10.1007/978-88-470-1935-5.

Anselmann, M. & Bause, M. (2020) Higher order Galerkin-collocation time discretization with Nitsche's method for the Navier–Stokes equations. *Math. Comput. Simul.* doi: 10.1016/j.matcom.2020.10.027.

Apel, T. (1999) *Anisotropic Finite Elements: Local Estimates and Applications*. Advances in Numerical Mathematics. Stuttgart: Teubner, ISBN: 3-519-02744-5.

Babuska, I. (1973) The finite element method with penalty. *Math. Comp.*, **27**, 221–228. doi: 10.1090/S0025-5718-1973-0351118-5.

Barrett, J. W. & Elliott, C. M. (1986) Finite element approximation of the Dirichlet problem using the boundary penalty method'. *Numer. Math.*, **49**, 343–366. doi: 10.1007/BF01389536.

Behr, M. (2001) Stabilized space-time finite element formulations for free-surface flows. *Commun. Numer. Methods Eng.*, **11**, 813–819. doi: 10.1002/cnm.451.

Behr, M. (2008) Simplex space-time meshes in finite element simulations. *Inter. J. Numer. Meth. Fluids*, **57**, 1421–1434. doi: 10.1002/fld.1796.

Besier, M. & Wollner, W. (2011) On the pressure approximation in nonstationary incompressible flow simulations on dynamically varying spatial meshes. *Internat. J. Numer. Methods Fluids*, **69**, 1045–1064. doi: 10.1002/fld.2625.

Brenner, A., Bansch, E. & Bause, M. (2013) A priori error analysis for finite element approximations of the Stokes problem on dynamic meshes. *IMA J. Numer. Anal.*, **34**, 123–146. doi: 10.1093/imanum/drt001.

Burman, E. (2010) Ghost penalty. *C.R. Math.*, **348**, 1217–1220. doi: 10.1016/j.crma.2010.10.006.

Burman, E., Frei, S. & Massing, A. (2019) Eulerian time-stepping schemes for the non-stationary Stokes equations on time-dependent domains. arXiv:1910.03054v1.

Burman, E. & Hansbo, P. (2012) Fictitious domain finite element methods using cut elements: II. A stabilized Nitsche method. *Appl. Numer. Math.*, **62**, 328–341. doi: 10.1016/j.apnum.2011.01.008.

Burman, E. & Hansbo, P. (2014) Fictitious domain methods using cut elements: III. A stabilized Nitsche method for Stokes' problem. *ESAIM Math. Model. Numer. Anal.*, **48**, 859–874. doi: 10.1051/m2an/2013123.

Burman, E., Claus, S., Hansbo, P., Larson, M. G. & Massing, M. (2014) CutFEM: discretizing geometry and partial differential equations. *Inter. J. Numer. Methods Engrg.*, **104**, 472–501. doi: 10.1002/nme.4823.

Donea, J., Giuliani, S. & Halleux, J. P. (1982) 'An arbitrary Lagrangian–Eulerian finite element method for transient dynamic fluid-structure interactions'. *In: Comput. Methods Appl. Mech. Engrg.*, **33**. 1–3, pp. 689–723. doi: 10.1016/0045-7825(82)90128-1.

Donea, J., Huerta, A., Ponthot, J.-Ph. & Rodríguez-Ferran, A. (2004) Arbitrary Lagrangian–Eulerian methods. *Encyclopedia of Computational Mechanics*. John Wiley & Sons, Ltd, . ISBN: 9780470091357. doi: 10.1002/0470091355.ecm009.

Ern, A. & Guermond, J.-L. (2004) *Theory and Practice of Finite Elements*. New York: Springer. doi: 10.1007/978-1-4757-4355-5.

Frei, S. & Richter, T. (2017) A second order time-stepping scheme for parabolic interface problems with moving interfaces. *ESAIM Math. Model. Numer. Anal.*, **51**, 1539–1560. doi: 10.1051/m2an/2016072.

Fries, T.-P. & Belytschko, T. (2010) The extended/generalized finite element method: an overview of the method and its applications. *Inter. J. Numer. Methods Engrg.*, **84**, 253–304. doi: 10.1002/nme.2914.

de Frutos, J., García-Archilla, B., John, V. & Novo, J. (2015) Grad-div Stabilization for the Evolutionary Oseen Problem with Inf-sup Stable Finite Elements. *In: J. Sci. Comput.*, **66**, 991–1024. doi: 10.1007/s10915-015-0052-1.

Glowinski, R., Pan, T.-W. & Periaux, J. (1994a) A fictitious domain method for Dirichlet problem and applications. *Comput. Methods Appl. Mech. Engrg.*, **111**, 283–303. ISSN: 0045-7825. doi: 10.1016/0045-7825(94)90135-X.

Glowinski, R., Pan, T.-W. & Periaux, J. (1994b) A fictitious domain method for external incompressible viscous flow modeled by Navier–Stokes equations. *Comput. Methods Appl. Mech. Engrg.*, **112**, 133–148. ISSN: 0045-7825. doi: 10.1016/0045-7825(94)90022-1.

Grande, J., Olshanskii, M. A. & Reusken, A. (2014) A space-time FEM for PDEs on evolving surfaces. *Proceedings of 11th World Congress on Computational Mechanics* (E. Onate, J. Oliver & A. Huerta eds). Eccomas. IGPM report 386 RWTH Aachen.

Gross, S., Olshanskii, M. A. & Reusken, A. (2014) A trace finite element method for a class of coupled bulk-interface transport problems. arXiv:1406.7694v2.

Gross, S., Olshanskii, M. A. & Reusken, A. (2015) A trace finite element method for a class of coupled bulkinterface transport problems. *ESAIM Math. Model. Numer. Anal.*, **49**, 1303–1330. doi: 10.1051/m2an/2015013.

Gürkan, C. & Massing, A. (2019) A stabilized cut discontinuous Galerkin framework for elliptic boundary value and interface problems. *Comput. Methods Appl. Mech. Engrg.*, **348**, 466–499. doi: 10.1016/j.cma.2018.12.041.

Guzmán, J. & Olshanskii, M. (2017) Inf-sup stability of geometrically unfitted Stokes finite elements. *Math. Comp.*, **87**, 2091–2112. doi: 10.1090/mcom/3288.

Hansbo, A. & Hansbo, P. (2002) An unfitted finite element method, based on Nitsche's method, for elliptic interface problems. *Comput. Methods Appl. Mech. Engrg.*, **191**, 5537–5552. doi: 10.1016/s0045-7825(02)00524-8.

Hansbo, P., Larson, M. G. & Zahedi, S. (2016) A cut finite element method for coupled bulk-surface problems on time-dependent domains. *Comput. Methods Appl. Mech. Engrg.*, **307**, 96–116. ISSN: 0045-7825. doi: 10.1016/j.cma.2016.04.012.

Heywood, J. G. & Rannacher, R. (1990) Finite-element approximation of the nonstationary Navier–Stokes problem. Part IV: error analysis for second-order time discretization. *SIAM J. Numer. Anal.*, **27**, 353–384. doi: 10.1137/0727022.

Intel (2019) *Intel Math Kernel Library*. https://software.intel.com/en-us/mkl.

John, V. (2016) *Finite element methods for incompressible flow problems*. Springer International Publishing. doi: 10.1007/978-3-319-45750-5.

Klaij, C., van der Vegt, J. & van der Ven, H. (2006) Space-time discontinuous Galerkin method for the compressible Navier–Stokes equations. *J. Comput. Phys.*, **217**, 589–611. ISSN: 0021–9991. doi: 10.1016/j.jcp.2006.01.018.

Lehrenfeld, C. (2015) The Nitsche XFEM-DG space-time method and its implementation in three space dimensions. *SIAM J. Sci. Comp.*, **37**, A245–A270. doi: 10.1137/130943534.

Lehrenfeld, C. (2016) High order unfitted finite element methods on level set domains using isoparametric mappings. *Comput. Methods Appl. Mech. Engrg.*, **300**, 716–733. doi: 10.1016/j.cma.2015.12.005.

Lehrenfeld, C., Heimann, F., Preuß, J. & von Wahl, H. (2021) ngsxfem: An add-on to NGSolve for unfitted finite element discretizations. *J. Open Source Softw*. doi: 10.21105/joss.03237.

Lehrenfeld, C. & Olshanskii, M. A. (2019) A Eulerian finite element method for PDEs in time-dependent domains. *ESAIM Math. Model. Numer. Anal.*, **53**, pp. 585–614. doi: 10.1051/m2an/2018068.

Lehrenfeld, C., Olshanskii, M. A. & Xu, X. (2018) A stabilized trace finite element method for partial differential equations on evolving surfaces. *SIAM J. Numer. Anal.*, **56**, 1643–1672. doi: 10.1137/17M1148633.

Lehrenfeld, C. & Reusken, A. (2013) Analysis of a Nitsche XFEM-DG discretization for a class of two-phase mass transport problems. *SIAM J. Numer. Anal.*, **51**, 958–983. doi: 10.1137/120875260.

Massing, A., Larson, M. G., Logg, A. & Rognes, M. E. (2014) A stabilized Nitsche fictitious domain method for the Stokes problem. *J. Sci. Comput.*, **61**, 604–628. doi: 10.1007/s10915-014-9838-9.

Neumüller, M. (2013) Space-time methods, fast solvers and applications. *Ph.D. Thesis*. Graz University of Technology. url: https://diglib.tugraz.at/download.php?id=576a7c40e7e04&location=browse (visited on 03/11/2020).

Nitsche, J. (1971) Über ein Variationsprinzip zur Lösung von Dirichlet-Problemen bei Verwendung von Teilräumen, die keinen Randbedingungen unterworfen sind'. *Abh. Math. Semin. Univ. Hambg.*, **36**, 9–15. doi: 10.1007/bf02995904.

Olshanskii, M. A. & Reusken, A. (2014) Error analysis of a space–time finite element method for solving PDEs on evolving surfaces. *SIAM J. Numer. Anal.*, **52**, 2092–2120. doi: 10.1137/130936877.

Olshanskii, M. A., Reusken, A. & Grande, J. (2009) A finite element method for elliptic equations on surfaces. *SIAM J. Numer. Anal.*, **47**, 3339–3358. doi: 10.1137/080717602.

Olshanskii, M. A., Reusken, A. & Xu, X. (2014) An Eulerian space–time finite element method for diffusion problems on evolving surfaces. *SIAM J. Numer. Anal.*, **52**, 1354–1377. doi: 10.1137/130918149.

Parvizian, J., Düster, A. & Rank, E. (2007) Finite cell method. *Comput. Mech.*, **41**, 121–133. ISSN: 0178-7675. doi: 10.1007/s00466-007-0173-y.

Peskin, C. S. & McQueen, D. M. (1989) A three-dimensional computational method for blood flow in the heart I. Immersed elastic fibers in a viscous incompressible fluid. *J. Comput. Phys.*, **81**, pp. 372–405. doi: 10.1016/0021-9991(89)90213-1.

Preuß, J. (2018) Higher order unfitted isoparametric space-time FEM on moving domains. *MA Thesis*. Georg-August Universität Göttingen. url: http://num.math.uni-goettingen.de/~lehrenfeld/sections/pubs_src/Pre18_Ma.pdf.

Quarteroni, A. (2014) *Numerical Models for Differential Problems*. Milan: Springer. doi: 10.1007/978-88-470-5522-3.

Richter, T. (2017) *Fluid–Structure Interactions. Models, Analysis and Finite Elements*, vol. **218**. Lecture Notes in Computational Science and Engineering. Cham: Springer. doi: 10.1007/978-3-319-63970-3.

Schöberl, J. (2014) C++11 implementation of finite elements in NGSolve. ASC Report No. 30/2014. *Technical Report Institute for Analysis and Scientific Computing*, TU Wien, 26th Sept. ISRN: 978–3–902627-05-6. url: http://www.asc.tuwien.ac.at/schoeberl/wiki/publications/ngs-cpp11.pdf.

Schöberl, J. (1997) NETGEN an advancing front 2D/3D-mesh generator based on abstract rules. *Comput. Vis. Sci.*, **1**, 41–52. doi: 10.1007/s007910050004.

Schott, B. (2017) Stabilized cut finite element methods for complex interface coupled flow problems. *Ph.D. Thesis*. Technischen Universität München. url: http://mediatum.ub.tum.de?id=1304754.

Schott, B. & Wall, W. A. (2014) A new face-oriented stabilized XFEM approach for 2D and 3D incompressible Navier–Stokes equations. *Comput. Methods Appl. Mech. Engrg.*, **276**, 233–265. doi: 10.1016/j.cma.2014.02.014.

Scott, R. & Zhang, S. (1990) Finite element interpolation of nonsmooth functions satisfying boundary conditions. *Math. Comp.*, **54**, 483–493. doi: 10.1090/s0025-5718-1990-1011446-7.

Sonner, F. & Richter, T. (2020) Second order pressure estimates for the Crank–Nicolson discretization of the incompressible Navier–Stokes equations. *SIAM J. Numer. Anal.*, **58**, 375–409. doi: 10.1137/18M1234813.

Stein, E. M. (1970) *Singular Integrals and Differentiability Properties of Functions*, vol. **30**. Princeton Mathematical Series. Princeton University Press. 304 pp. ISBN: 0-691-08079-8.

Temem, R. (1982) Behaviour at time $t = 0$ of the solutions of semi-linear evolution equations. *J. Differ. Equ.*, **43**, 73–92. doi: 10.1016/0022-0396(82)90075-4.

Voulis, I. & Reusken, A. (2018) A time dependent Stokes interface problem: well-posedness and space-time finite element discretization. *ESAIM Math. Model. Numer. Anal.*, **52**, 2187–2213. doi: 10.1051/m2an/2018053.

von Wahl, H., Richter, T. & Lehrenfeld, C. (2020) An unfitted Eulerian finite element method for the time-dependent Stokes problem on moving domains. arXiv:2002.02352v1.

Zahedi, S. (2018) A space-time cut finite element method with quadrature in time. *Geometrically Unfitted Finite Element Methods and Applications—Proceedings of the UCL Workshop 2016*. Lecture Notes in Computational Science and Engineering. Cham: Springer. doi: 10.1007/978-3-319-71431-8_9.